J. Appl. Comput. Mech., 7(1) (2021) 189-212
DOI: 10.22055/JACM.2020.34930.2514

ISSN: 2383-4536
jacm.scu.ac.ir

Shahid Chamran University of Ahvaz

Journal of Applied and Computational Mechanics

Research Paper

Heat and Mass Transfer of Natural Convective Flow with Slanted Magnetic Field via Fractional Operators

Nazish Iftikhar[1], Dumitru Baleanu[2,3,4], Muhammad Bilal Riaz[5,6], Syed Muhammad Husnine[1]

[1] Department of Science & Humanities, National University of Computer and Emerging Sciences,
Lahore Campus, 54000, Pakistan, Emails: nazish.iftikhar289@gmail.com, syed.husnine@nu.edu.pk
[2] Department of Mathematics, Cankaya University, Ankara, 06790, Turkey, Email: dumitru@cankaya.edu.tr
[3] Institute of Space Sciences, Magurele, Bucharest, 077125, Romania
[4] Department of Medical Research, China Medical University Hospital, China Medical University, Taichung City, 40402, Taiwan
[5] Department of Mathematics, University of Management and Technology, Lahore, 54000, Pakistan, Email: bilalsehole@gmail.com
[6] Institute for Groundwater Studies (IGS), University of the Free State, Bloemfontein, 9301, South Africa

Received September 07 2020; Revised September 25 2020; Accepted for publication September 28 2020.
Corresponding author: D. Baleanu (dumitru@cankaya.edu.tr)

Abstract. This article explores the MHD natural convective viscous and incompressible fluid flow along with radiation and chemical reaction. The flow is confined to a moving tilted plate under slanted magnetic field with variable temperature in a porous medium. Non-dimensional parameter along Laplace transformation and inversion algorithm are used to investigate the solution of system of dimensionless governing equations. Fractional differential operators namely, Caputo (C), Caputo-Fabrizio (CF) and Atangana-Baleanu in Caputo sense (ABC) are used to compare graphical behavior of for velocity, temperature and concentration for emerging parameters. On comparison, it is observed that fractional order model is better in explaining the memory effect as compared to classical model. Velocity showing increasing behavior for fractional parameter α whereas there is a decline in temperature, and concentration profiles for α. Fluid velocity goes through a decay due to rise in the values of M, Sc and φ. However, velocity shows a reverse profile for augmented inputs of K_p, G_r and S. Tabular comparison is made for velocity and Nusselt number and Sherwood number for fractional models.

Keywords: Fractional order derivatives; Inclined magnetic field; Laplace transformation; Inversion algorithm.

1. Introduction

The viscoelastic fluids gain attention in many fields of science and engineering. MHD natural convection flow of a viscous and incompressible fluid involving heat and mass transfer phenomena has been focused by researchers due to its several practical applications like crystal formation, grain storage, high performance insulation for buildings, and geothermal energy systems etc. Some significant efforts have been made by investigators for study of heat and mass transfer in viscous fluid [1] – [4]. Derivatives play a significant role in modeling mathematical problems. Fractional derivatives, as compared to ordinary derivatives, are more applicable in different fields like fluid mechanics, engineering, chemical industry, Chaotic and fractional attractors, and many more [5] – [11].

Fractional calculus plays a key role in describing the behavior of viscoelastic fluids [12] – [13]. Generally, ordinary derivative is replaced by fractional order derivative in governing equations [14]. Fractional order fluid models have been discussed by many researchers [15] – [24]. The natural convection flow of an MHD viscous fluid over a slanted heated surface has many applications in astronomy, cooling towers, geophysics, and boundary layer problems. Umemura and Law [25] discussed the free natural convection flow on a semi-infinite heated plate of different inclination. Analysis of heat and mass transfer of convective flow in a permeable medium over a titled moving plate discussed by Pattnaik et al. [26]. Nandkeolyar and Das [27] studied free convection flow with radiative heat under slanted magnetic field in the permeable medium. Endalew and Nayak [28] focused on MHD natural convective flow with radiation and chemical reaction with tilted magnetic field on a slanted moving plate. Study regarding free convective flow through permeable medium past an inclined plate can be seen through [29] – [30]. Makinde [31] worked on the mixed convection stagnation point flow with porosity effect radiation. Khalid et al. [32] studies the Casson fluid flow past a moving plate via a porous medium with constant temperature on the wall. Moreover, some important results show in [33] – [36].

Fractional derivatives play a significant role in heat and mass transfer phenomenon. Shah et al. [37] investigated heat and mass transfer phenomena of natural convection viscous flow with Dufour effect via Caputo fractional derivative. Heat and mass transfer phenomena in Maxwell fluid via CF and ABC approach has been discussed by Khan et al. [38]. Tassaddiq [39] explores second grade fluid with tilted plate and slanted magnetic field by ABC approach. Free convection MHD viscous fluid flow near a

Published online: September 29 2020

vertical plate and constant heat through Caputo time-fractional derivative has been discussed by Shah et al. [40]. Momentum and heat transfer analysis for MHD second grade fluid enclosed in a permeable medium through Caputo-Fabrzio derivative has been investigated by Sheikh [41]. Imran et al. [42] discussed MHD free convection flow of Newtonian fluid on an inclined plate through porous medium with variable temperature and concentration at the boundary via CF and ABC. Ahmad et al. [43] studied heat and mass transfer of fractional Jeffrey flow over infinite vertical plate moving exponentially with variable temperature and mass diffusion using C and CF. In literature, problems based on fractional order derivatives have been focused by many researchers [44] – [48]. In the paper, viscous fluid flow past a moving tilted plate has been taken into account. Furthermore, slanted magnetic field is applied with addition to radiation and chemical reaction in a permeable medium by using definitions of integer order and fractional derivatives.

2. Problem Statement

Let natural convective flow of the viscous fluid past an infinite titled plate with slanted magnetic field $B=(B_0 Cos\phi, B_0 Sin\phi, 0)$ makes an angle ϕ with vertical. Let the plate is slanted and makes an angle θ with the vertical. At the start, fluid and plate exhibit concentration C'_∞ and temperature T'_∞. Velocity of plate is given by $W'=U_0(a't')$. Figure 1 presents the geometry of fluid flow [28].

$$\frac{\partial W'(\psi',t')}{\partial t'}=\upsilon\frac{\partial^2 W'(\psi',t')}{\partial \psi'^2}+g\beta_T(T'(\psi',t')-T'_\infty)Cos\theta+g\beta_C(C'(\psi',t')-C'_\infty)Cos\theta-\left(\frac{\sigma B_0^2 Sin^2\phi}{\rho}+\frac{\upsilon}{K'_p}\right)W'(\psi',t'), \tag{1}$$

$$\rho c_p\frac{\partial T'(\psi',t')}{\partial t'}=k\frac{\partial^2 T'(\psi',t')}{\partial \psi'^2}-\frac{\partial q_r}{\partial \psi'}+S'(T'(\psi',t')-T'_\infty), \tag{2}$$

$$D\frac{\partial^2 C'(\psi',t')}{\partial \psi'^2}-K'_c(C'(\psi',t')-C'_\infty). \tag{3}$$

The suitable initial as well as boundary conditions are

$$t'\le 0,\quad W'=0,\quad T'=T'_\infty,,\quad C'=C'_\infty,\quad \forall \quad \psi',$$

$$t'>0,\quad W'=U_0(a't'),\quad T'=T'_\infty+\frac{(T'_w-T'_\infty)U_0{}^2t'}{\upsilon},\quad C'=C'_\infty+\frac{(C'_w-C'_\infty)U_0{}^2t'}{\upsilon},\quad \psi'=0,$$

$$t'>0,\quad W'\to 0,\quad T'\to T'_\infty,\quad C'\to C'_\infty,\quad \psi'\to\infty,$$

where

$$\frac{\partial q_r}{\partial \psi'}=-(T'^4_\infty-T'^4)4a^*\sigma,\qquad T'^4=-3T'^4_\infty+4T'^3_\infty T'.$$

Equation (1 – 3) can be non-dimensionalized by dimensionless variables as follow:

$$\psi=\frac{U_0}{\upsilon}\psi',\quad W=\frac{W'}{U_0},\quad t=\frac{t'U_0{}^2}{\upsilon},\quad a=\frac{a'\nu}{U_0{}^2},\quad T=\frac{T'-T'_\infty}{T'_w-T'_\infty},\quad C=\frac{C'-C'_\infty}{C'_w-C'_\infty},\quad K_c=\frac{\upsilon K_c{}'}{U_0{}^2},$$

$$K_p=\frac{U_0{}^2K_p{}'}{\upsilon^2},\quad S=\frac{S'\nu}{\rho C_p U_0{}^2},\quad Sc=\frac{\upsilon}{D},\quad Pr=\frac{\mu Cp}{k},\quad G_r=\frac{g\beta_T\nu(T'_w-T'_\infty)}{U_0{}^3},\quad M=\frac{\sigma B_0^2\upsilon}{\rho U_0^2}, \tag{5}$$

$$G_r=\frac{g\beta_T\nu(T'_w-T'_\infty)}{U_0{}^3},\quad G_c=\frac{g\beta_c\nu(C'_w-C'_\infty)}{U_0{}^3},\quad R=\frac{16a^*\nu^2\sigma T'^3_\infty}{kU_0{}^2}.$$

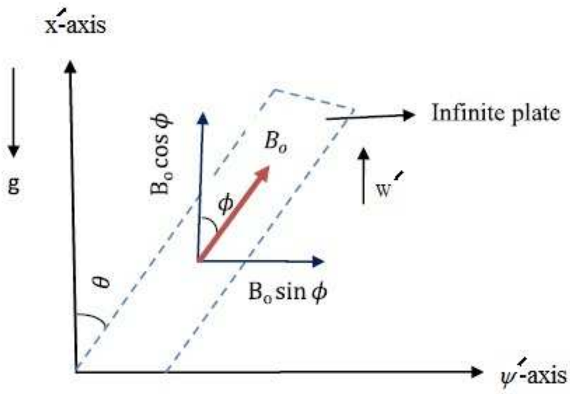

Fig. 1. Geometrical presentation of fluid model

Governing equations with corresponding IBC transformed into

$$\frac{\partial W(\psi,t)}{\partial t}=\frac{\partial^2 W(\psi,t)}{\partial\psi^2}-\lambda W(\psi,t)+G_r Cos\theta T(\psi,t)+G_c Cos\theta C(\psi,t), \tag{6}$$

$$Pr\frac{\partial T(\psi,t)}{\partial t}=\frac{\partial^2 T(\psi,t)}{\partial\psi^2}-dT(\psi,t), \tag{7}$$

$$Sc\frac{\partial C(\psi,t)}{\partial t}=\frac{\partial^2 C(\psi,t)}{\partial\psi^2}-ScK_c C(\psi,t), \tag{8}$$

where

$$\lambda=MSin^2\phi+\frac{1}{K_p},\quad d=R-SPr,$$

with initial and boundary conditions:

$$\begin{aligned} &t\le 0,\quad W=0,\quad T=0,\quad C=0,\quad \psi>0,\\ &t>0,\quad W=at,\quad T=t,\quad C=t,\quad \psi=0,\\ &t>0,\quad W\to 0,\quad T\to 0,\quad C\to 0,\quad \psi\to\infty. \end{aligned} \tag{9}$$

3. Preliminaries

Caputo time derivative [16] with its Laplace transform (LT) with $\Gamma(.)$ gamma function is given below

$${}^{C}D_t^{\eta}\gamma(\psi,t)=\frac{1}{\Gamma(n-\eta)}\int_0^t\left(\frac{\gamma^{n}(\tau)}{(t-\tau)^{\eta+1-n}}\right)d\tau, \tag{10}$$

$$L\left({}^{C}D_t^{\eta}\gamma(\psi,t)\right)=s^{\eta}L(\gamma(\psi,t))-s^{\eta-1}\gamma(\psi,0). \tag{11}$$

The CF fractional derivative and its LT are defined as [44] and [45]

$${}^{CF}D_t^{\eta}\gamma(\psi,t)=\frac{1}{1-\eta}\int_0^t\exp\left(-\frac{\eta(t-\tau)}{1-\eta}\right)\frac{\partial\gamma(\psi,\tau)}{\partial\tau}d\tau,\qquad 0<\eta<1, \tag{12}$$

$$L\left({}^{CF}D_t^{\eta}\gamma(\psi,t)\right)=\frac{sL(\gamma(\psi,t))-\gamma(\psi,0)}{(1-\eta)s+\eta}. \tag{13}$$

The ABC fractional derivative and its LT are defined as [45] and [46] is given by

$${}^{ABC}D_t^{\eta}\gamma(\psi,t)=\frac{1}{1-\eta}\int_0^t E_{\eta}\left(-\frac{\eta(t-\tau)}{1-\eta}\right)\frac{\partial\gamma(\psi,\tau)}{\partial\tau}d\tau, \tag{14}$$

$$L\left({}^{ABC}D_t^{\eta}\gamma(\psi,t)\right)=\frac{s^{\eta}L(\gamma(\psi,t))-s^{\eta-1}\gamma(\psi,0)}{(1-\eta)s^{\eta}+\eta}. \tag{15}$$

4. Solutions for Temperature Profile

4.1 Integer Order Derivative

Laplace transform of equation (7) is

$$Pr\,m\bar{T}(\psi,m)=\frac{\partial^2\bar{T}(\psi,m)}{\partial\psi^2}-d\bar{T}(\psi,m), \tag{16}$$

Laplace solution of equation (16) is

$$\bar{T}(\psi,m)=\frac{1}{m^2}e^{-\psi\sqrt{prm+d}}. \tag{17}$$

4.2 Caputo Fractional Derivative

Applying Caputo definition (10) to equation (7), we get

$$\Pr {}^{C}D_t^{\alpha}T_c(\psi,t)=\frac{\partial^2 T_c(\psi,t)}{\partial\psi^2}-dT_c(\psi,t), \tag{18}$$

employing Laplace transformation on (7) with the help of (11), we explored second order partial differential equation,

$$\Pr m^{\alpha}\overline{T}_c(\psi,m)=\frac{\partial^2 \overline{T}_c(\psi,m)}{\partial\psi^2}-d\overline{T}_c(\psi,m). \tag{19}$$

Solution of the above equation is

$$\overline{T}_c(\psi,m)=\frac{1}{m^2}e^{-\psi\sqrt{prm^{\alpha}+d}}. \tag{20}$$

4.3 Caputo-Fabrizio Fractional Derivative

Temperature field obtained by using (12) to (7)

$$\Pr {}^{CF}D_t^{\alpha}T_{cf}(\psi,t)=\frac{\partial^2 T_{cf}(\psi,t)}{\partial\psi^2}-dT_{cf}(\psi,t), \tag{21}$$

The Laplace transform of above equation is

$$\Pr\left(\frac{m}{(1-\alpha)m+\alpha}\right)\overline{T}_{cf}(\psi,m)=\frac{\partial^2 \overline{T}_{cf}(\psi,m)}{\partial\psi^2}-d\overline{T}_{cf}(\psi,m). \tag{22}$$

Solution of the above mentioned equation is

$$\overline{T}_{cf}(\psi,m)=\frac{1}{m^2}e^{-\psi\sqrt{\frac{(a_0\Pr+d)m+a_1 d}{m+a_1}}}, \tag{23}$$

where $a_0=1/(1-\alpha)$ and $a_1=\alpha a_0$.

4.4 Atangana-Baleanu Fractional Derivative

ABC version of equation (7) is

$$\Pr {}^{ABC}D_t^{\alpha}T_{abc}(\psi,t)=\frac{\partial^2 T_{abc}(\psi,t)}{\partial\psi^2}-dT_{abc}(\psi,t), \tag{24}$$

Applying definition of ABC-fractional derivative defined as [14] to above equation, we get

$$\Pr\left(\frac{m^{\alpha}}{(1-\alpha)m^{\alpha}+\alpha}\right)\overline{T}_{abc}(\psi,m)=\frac{\partial^2 \overline{T}_{abc}(\psi,m)}{\partial\psi^2}-d\overline{T}_{abc}(\psi,m). \tag{25}$$

Solution of equation (25) is given as

$$\overline{T}_{abc}(\psi,m)=\frac{1}{m^2}e^{-\psi\sqrt{\frac{(a_0\Pr+d)m^{\alpha}+a_1 d}{m^{\alpha}+a_1}}}. \tag{26}$$

5. Solutions for Concentration Profile

5.1 Integer Order Derivative

Laplace transform of equation (8) is

$$Scm\overline{C}(\psi,m)=\frac{\partial^2 \overline{C}(\psi,m)}{\partial\psi^2}-K_c Sc\overline{C}(\psi,m), \tag{27}$$

solution of the above equation is given as

$$\overline{C}(\psi,m)=\frac{1}{m^2}e^{-\psi\sqrt{Sc(m+K_c)}}. \tag{28}$$

5.2 Caputo Fractional Derivative

Applying Caputo definition (10) to equation (8), we get

$$Sc {}^{C}D_t^{\alpha}C_c(\psi,t)=\frac{\partial^2 C_c(\psi,t)}{\partial\psi^2}-K_c ScC_c(\psi,t), \tag{29}$$

employing Laplace transformation on (8) with the help of (11), we explored second order partial differential equation,

$$Scm^{\alpha}\overline{C}_c(\psi,m)=\frac{\partial^2 \overline{C}_c(\psi,m)}{\partial\psi^2}-K_c Sc\overline{C}_c(\psi,m). \tag{30}$$

Solution of the above equation is

$$\bar{C}_c(\psi,m)=\frac{1}{m^2}e^{-\psi\sqrt{Sc(m^\alpha+K_c)}}. \tag{31}$$

5.3 Caputo-Fabrizio Fractional Derivative

Concentration field obtained by using (12) to (8)

$$Sc\,{}^{CF}D_t^\alpha C_{cf}(\psi,t)=\frac{\partial^2 C_{cf}(\psi,t)}{\partial\psi^2}-K_cScC_{cf}(\psi,t). \tag{32}$$

The Laplace transform of above equation is

$$Sc\left(\frac{m}{(1-\alpha)m+\alpha}\right)\bar{C}_{cf}(\psi,m)=\frac{\partial^2\bar{C}_{cf}(\psi,m)}{\partial\psi^2}-K_cSc\bar{C}_{cf}(\psi,m). \tag{33}$$

Solution of the above mentioned equation is

$$\bar{C}_{cf}(\psi,m)=\frac{1}{m^2}e^{-\psi\sqrt{\frac{Sc(a_0+K_c)m+a_1K_cSc}{m+a_1}}}. \tag{34}$$

5.4 Atangana-Baleanu Fractional Derivative

ABC version of equation (8) is

$$Sc\,{}^{ABC}D_t^\alpha C_{abc}(\psi,t)=\frac{\partial^2 C_{abc}(\psi,t)}{\partial\psi^2}-K_cScC_{abc}(\psi,t). \tag{35}$$

Applying definition of ABC-fractional derivative defined as [14] to above equation, we get

$$Sc\left(\frac{m^\alpha}{(1-\alpha)m^\alpha+\alpha}\right)\bar{C}_{abc}(\psi,m)=\frac{\partial^2\bar{C}_{abc}(\psi,m)}{\partial\psi^2}-K_cSc\bar{C}_{abc}(\psi,m). \tag{36}$$

Solution of equation (36) is given as

$$\bar{C}_{abc}(\psi,m)=\frac{1}{m^2}e^{-\psi\sqrt{\frac{Sc(a_0+K_c)m^\alpha+a_1K_cSc}{m^\alpha+a_1}}}, \tag{37}$$

6. Solution for Velocity Field

6.1 Integer Order Derivative

By applying Laplace transform to equation (6) and after some simplification, we get

$$\frac{\partial^2\bar{W}(\psi,m)}{\partial\psi^2}-(m+\lambda)\bar{W}(\psi,m)=-G_rCos\theta\bar{T}(\psi,m)-G_cCos\theta\bar{C}(\psi,m), \tag{38}$$

puttting the value of $\bar{T}(\psi,m)$ from (17) and $\bar{C}(\psi,m)$ from (28) in (38), we have

$$\frac{\partial^2\bar{W}(\psi,m)}{\partial\psi^2}-(m+\lambda)\bar{W}(\psi,m)=-G_rCos\theta\left(\frac{1}{m^2}e^{-\psi\sqrt{prm+d}}\right)-G_cCos\theta\left(\frac{1}{m^2}e^{-\psi\sqrt{Sc(m+K_c)}}\right). \tag{39}$$

The solution of the equation (39) is given by

$$\begin{aligned}\bar{W}(\psi,m)=&\frac{a}{m^2}e^{-\psi\sqrt{m+\lambda}}+\frac{G_rCos\theta}{d-\lambda}\left(e^{-\psi\sqrt{m+\lambda}}-e^{-\psi\sqrt{\Pr m+d}}\right)\left(\frac{1-\Pr}{m(d-\lambda)}+\frac{1}{m^2}+\frac{1}{(d-\lambda)(m(\Pr-1)+(d-\lambda))}\right)\\&+\frac{G_cCos\theta}{K_cSc-\lambda}\left(e^{-\psi\sqrt{m+\lambda}}-e^{-\psi\sqrt{Sc(m+K_c)}}\right)\left(\frac{1-Sc}{m(K_cSc-\lambda)}+\frac{1}{m^2}+\frac{1}{(K_cSc-\lambda)(m(Sc-1)+(K_cSc-\lambda))}\right).\end{aligned} \tag{40}$$

6.2 Caputo Fractional Derivative

Velocity equation (6) with reference to Caputo definition (10) is given by

$${}^{C}D_t^\alpha W_c(\psi,t)=\frac{\partial^2 W_c(\psi,t)}{\partial\psi^2}-\lambda W_c(\psi,t)+G_rCos\theta T_c(\psi,t)+G_cCos\theta C_c(\psi,t), \tag{41}$$

employing Laplace transformation on (6) with the help of (11), we explored second order partial differential equation,

$$\frac{\partial^2\bar{W}_c(\psi,m)}{\partial\psi^2}-(m^\alpha+\lambda)\bar{W}_c(\psi,m)=-G_rCos\theta\bar{T}_c(\psi,m)-G_cCos\theta\bar{C}_c(\psi,m), \tag{42}$$

puttting the value of $\bar{T}_c(\psi,m)$ from (20) and $\bar{C}_c(\psi,m)$ from (31) in (42), we have

$$\frac{\partial^2\bar{W}_c(\psi,m)}{\partial\psi^2}-\left(m^\alpha+\lambda\right)\bar{W}_c(\psi,m)=-G_r Cos\theta\left(\frac{1}{m^2}e^{-\psi\sqrt{prm^\alpha+d}}\right)-G_c Cos\theta\left(\frac{1}{m^2}e^{-\psi\sqrt{Sc\left(m^\alpha+K_c\right)}}\right). \tag{43}$$

The solution of the equation (43) is given by

$$\begin{aligned}\bar{W}_c(\psi,m)=&\frac{a}{m^2}e^{-\psi\sqrt{m^\alpha+\lambda}}+\frac{G_r Cos\theta}{d-\lambda}\left(e^{-\psi\sqrt{m^\alpha+\lambda}}-e^{-\psi\sqrt{\Pr m^\alpha+d}}\right)\left(\frac{1-\Pr}{m^\alpha(d-\lambda)}+\frac{1}{m^2}+\frac{1}{(d-\lambda)\left(m^\alpha(\Pr-1)+(d-\lambda)\right)}\right)\\&+\frac{G_c Cos\theta}{K_c Sc-\lambda}\left(e^{-\psi\sqrt{m^\alpha+\lambda}}-e^{-\psi\sqrt{Sc\left(m^\alpha+K_c\right)}}\right)\left(\frac{1-Sc}{m^\alpha(K_c Sc-\lambda)}+\frac{1}{m^2}+\frac{1}{(K_c Sc-\lambda)\left(m^\alpha(Sc-1)+(K_c Sc-\lambda)\right)}\right).\end{aligned} \tag{44}$$

6.3 Caputo-Fabrizio Fractional Derivative

Velocity equation (6) with reference to Caputo definition (12) is given by

$$^{CF}D_t^\alpha W_{cf}(\psi,t)=\frac{\partial^2 W_{cf}(\psi,t)}{\partial\psi^2}-\lambda W_{cf}(\psi,t)+G_r Cos\theta T_{cf}(\psi,t)+G_c Cos\theta C_{cf}(\psi,t), \tag{45}$$

employing Laplace transformation on (6) with the help of (13), we explored second order partial differential equation,

$$\frac{\partial^2\bar{W}_{cf}(\psi,m)}{\partial\psi^2}-\left(m^\alpha+\lambda\right)\bar{W}_{cf}(\psi,m)=-G_r Cos\theta\bar{T}_{cf}(\psi,m)-G_c Cos\theta\bar{C}_{cf}(\psi,m), \tag{46}$$

puttting the value of $\bar{T}_{cf}(\psi,m)$ from (23) and $\bar{C}_{cf}(\psi,m)$ from (34) in (46), we have

$$\frac{\partial^2\bar{W}_{cf}(\psi,m)}{\partial\psi^2}-\left(m^\alpha+\lambda\right)\bar{W}_{cf}(\psi,m)=-G_r Cos\theta\left(\frac{1}{m^2}e^{-\psi\sqrt{\frac{(a_0\Pr+d)m+a_1d}{m+a_1}}}\right)-G_c Cos\theta\left(\frac{1}{m^2}e^{-\psi\sqrt{\frac{Sc(a_0+K_c)m+a_1K_cSc}{m+a_1}}}\right). \tag{47}$$

The solution of the equation (47) is given by

$$\begin{aligned}\bar{W}_{cf}(\psi,m)=&\frac{a}{m^2}e^{-\psi\sqrt{\frac{(a_0+\lambda)m+\lambda a_1}{m+a_1}}}+\frac{(m+a_1)G_r Cos\theta}{a_1(d-\lambda)}\left(e^{-\psi\sqrt{\frac{(a_0+\lambda)m+\lambda a_1}{m+a_1}}}-e^{-\psi\sqrt{\frac{(a_0\Pr+d)m+a_1d}{m+a_1}}}\right)\\&\times\left(\frac{\lambda-d-a_0(\Pr-1)}{m(d-\lambda)}+\frac{1}{m^2}+\frac{1}{a_1(d-\lambda)\left(m\left(a_0(\Pr-1)+d-\lambda\right)+a_1(d-\lambda)\right)}\right)\\&+\frac{(m+a_1)G_c Cos\theta}{a_1(K_cSc-\lambda)}\left(e^{-\psi\sqrt{\frac{(a_0+\lambda)m+\lambda a_1}{m+a_1}}}-e^{\psi\sqrt{\frac{Sc(a_0+K_c)m+a_1K_cSc}{m+a_1}}}\right)\\&\times\left(\frac{\lambda+a_0-Sc(a_0+K_c)}{ma_1(K_cSc-\lambda)}+\frac{1}{m^2}+\frac{1}{a_1(K_cSc-\lambda)\left(m\left(Sc(a_0+K_c)-a_0-\lambda\right)+a_1(K_cSc-\lambda)\right)}\right).\end{aligned} \tag{48}$$

6.4 Atangana-Baleanu Fractional Derivative

Velocity equation (6) with reference to ABC definition (14) is given by

$$^{ABC}D_t^\alpha W_{abc}(\psi,t)=\frac{\partial^2 W_{abc}(\psi,t)}{\partial\psi^2}-\lambda W_{abc}(\psi,t)+G_r Cos\theta T_{abc}(\psi,t)+G_c Cos\theta C_{abc}(\psi,t), \tag{49}$$

employing Laplace transformation on (6) with the help of (15), we explored second order partial differential equation,

$$\frac{\partial^2\bar{W}_{abc}(\psi,m)}{\partial\psi^2}-\left(\frac{(a_0+\lambda)m^\alpha+\lambda\alpha a_0}{m^\alpha+a_1}\right)\bar{W}_{abc}(\psi,m)=-G_r Cos\theta\bar{T}_{abc}(\psi,m)-G_c Cos\theta\bar{C}_{abc}(\psi,m), \tag{50}$$

puttting the value of $\bar{T}_{abc}(\psi,m)$ from (26) and $\bar{C}_{abc}(\psi,m)$ from (37) in (50), we have

$$\frac{\partial^2\bar{W}_{abc}(\psi,m)}{\partial\psi^2}-\left(m^\alpha+\lambda\right)\bar{W}_{abc}(\psi,m)=-G_r Cos\theta\left(\frac{1}{m^2}e^{-\psi\sqrt{\frac{(a_0\Pr+d)m^\alpha+a_1d}{m^\alpha+a_1}}}\right)-G_c Cos\theta\left(\frac{1}{m^2}e^{-\psi\sqrt{\frac{Sc(a_0+K_c)m^\alpha+a_1K_cSc}{m^\alpha+a_1}}}\right). \tag{51}$$

The required solution is

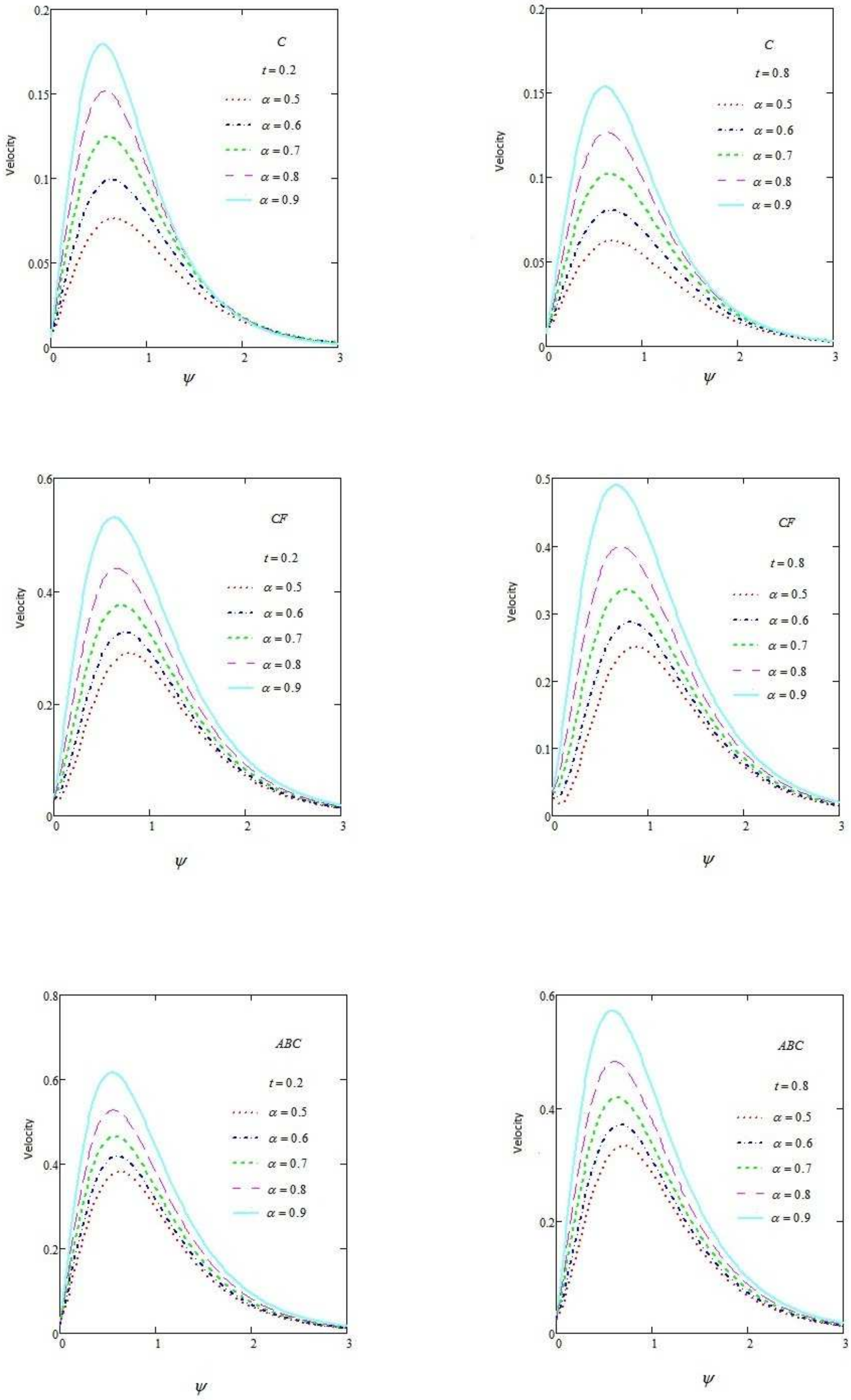

Fig. 2. Velocity curves for C, CF and ABC with variation in α where $G_r = 1, \Pr = 8, G_c = 1, Sc = 6, K_p = 0.5, K_c = 3, M = 1, R = 3, S = 0.5, a = 0.01,\ \theta = \frac{\pi}{3}, \phi = \frac{\pi}{4}$

$$
\begin{aligned}
\bar{W}_{abc}(\psi,m) &= \frac{a}{m^2} e^{-\psi\sqrt{\frac{(a_0+\lambda)m^\alpha+\lambda a_1}{m^\alpha+a_1}}} + \frac{(m^\alpha+a_1)G_r \mathrm{Cos}\theta}{a_1(d-\lambda)}\left(e^{-\psi\sqrt{\frac{(a_0+\lambda)m^\alpha+\lambda a_1}{m^\alpha+a_1}}} - e^{-\psi\sqrt{\frac{(a_0\Pr+d)m^\alpha+a_1 d}{m^\alpha+a_1}}}\right)\\
&\times\left(\frac{\lambda-d-a_0(\Pr-1)}{m^\alpha(d-\lambda)}+\frac{1}{m^2}+\frac{1}{a_1(d-\lambda)\left(m^\alpha\left(a_0(\Pr-1)+d-\lambda\right)+a_1(d-\lambda)\right)}\right)\\
&+\frac{(m^\alpha+a_1)G_c \mathrm{Cos}\theta}{a_1(K_c Sc-\lambda)}\left(e^{-\psi\sqrt{\frac{(a_0+\lambda)m^\alpha+\lambda a_1}{m^\alpha+a_1}}} - e^{\psi\sqrt{\frac{Sc(a_0+K_c)m^\alpha+a_1 K_c Sc}{m^\alpha+a_1}}}\right)\\
&\times\left(\frac{\lambda+a_0-Sc(a_0+K_c)}{m^\alpha a_1(K_c Sc-\lambda)}+\frac{1}{m^2}+\frac{1}{a_1(K_c Sc-\lambda)\left(m^\alpha\left(Sc(a_0+K_c)-a_0-\lambda\right)+a_1(K_c Sc-\lambda)\right)}\right).
\end{aligned}
\tag{52}
$$

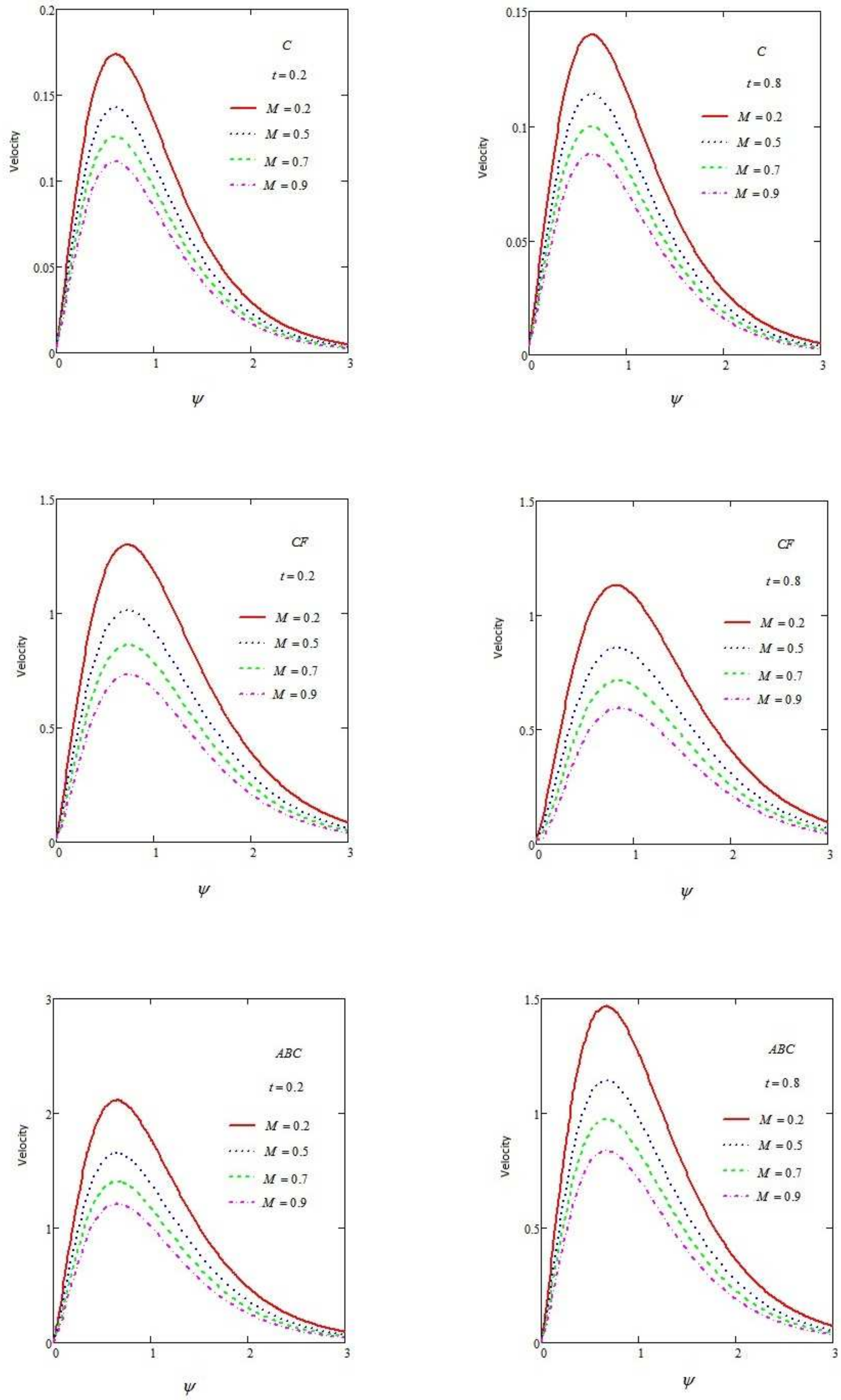

Fig. 3. Velocity curves for C, CF and ABC with variation in M where $G_r = 1, \Pr = 8, G_c = 1, Sc = 6, K_p = 0.5, K_c = 3, \alpha = 0.01, R = 3, S = 0.5, a = 0.01, \theta = \frac{\pi}{3}, \phi = \frac{\pi}{4}$

As $\alpha \to 1$, results are obtained present in Endalew et al. [28].
We apply Laplace transform to our flow model using fractional order derivatives and to approximates inverse Laplace transform, Stehfest's formula is one of the simplest algorithm that is why in the present work we apply the Stehfest's algorithm [49],[50] to sort out the inverse Laplace transform.

$$W(r,t) = \frac{e^{4.7}}{t}\left[\frac{1}{2}\bar{W}\left(r,\frac{4.7}{t}\right) + \mathrm{Re}\left\{\sum_{k=1}^{N_1}(-1)^k \bar{W}\left(r,\frac{k\pi i + 4.7}{t}\right)\right\}\right], \tag{53}$$

where N_1 is a natural number, $\mathrm{Re}(.)$ is a real part, and i is the imaginary unit [50].

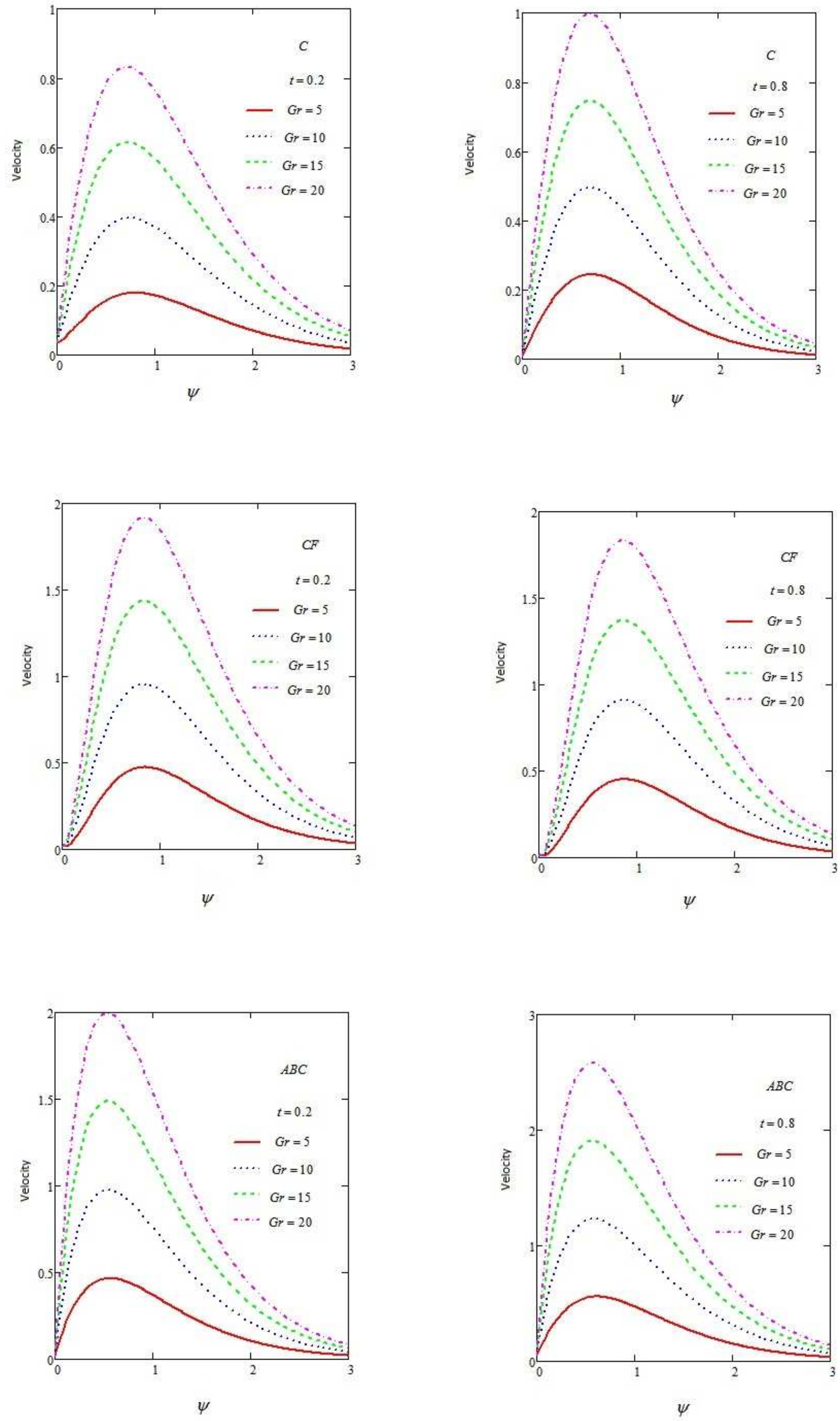

Fig. 4. Velocity curves for C, CF and ABC with variation in G_r where

$$M = 1, Pr = 8, G_c = 1, Sc = 6, K_p = 0.5, K_c = 3, \alpha = 0.01, R = 3, S = 0.5, a = 0.01, \theta = \frac{\pi}{3}, \phi = \frac{\pi}{4}$$

7. Results & Discussion

Comparative study of flow of natural convective flow over a moving slanted plate by applying inclined magnetic field with porosity is carried out with variable temperature. Momentum, heat and mass profiles are taken into account under the fractional operators C, CF and ABC. Graphical and tabular analysis has been illustrated for temperature, concentration and velocity for several emerging parameters $\alpha, M, G_r, Sc, K_p, K_c, R, S, Pr$ and ϕ using C, CF and ABC fractional operators.

7.1 Velocity profile for α

Figure (2) characterizes the control of fractional parameter on fluid flow. The velocity profile get accelerated with the increment in values of α. From the physical perspective, boundary layer thickness grows with increment in time as the result velocity is highest near plate. As $\alpha \rightarrow 1$, velocity curves approach to integer order which is the best explanation of fractional derivative for memory effect.

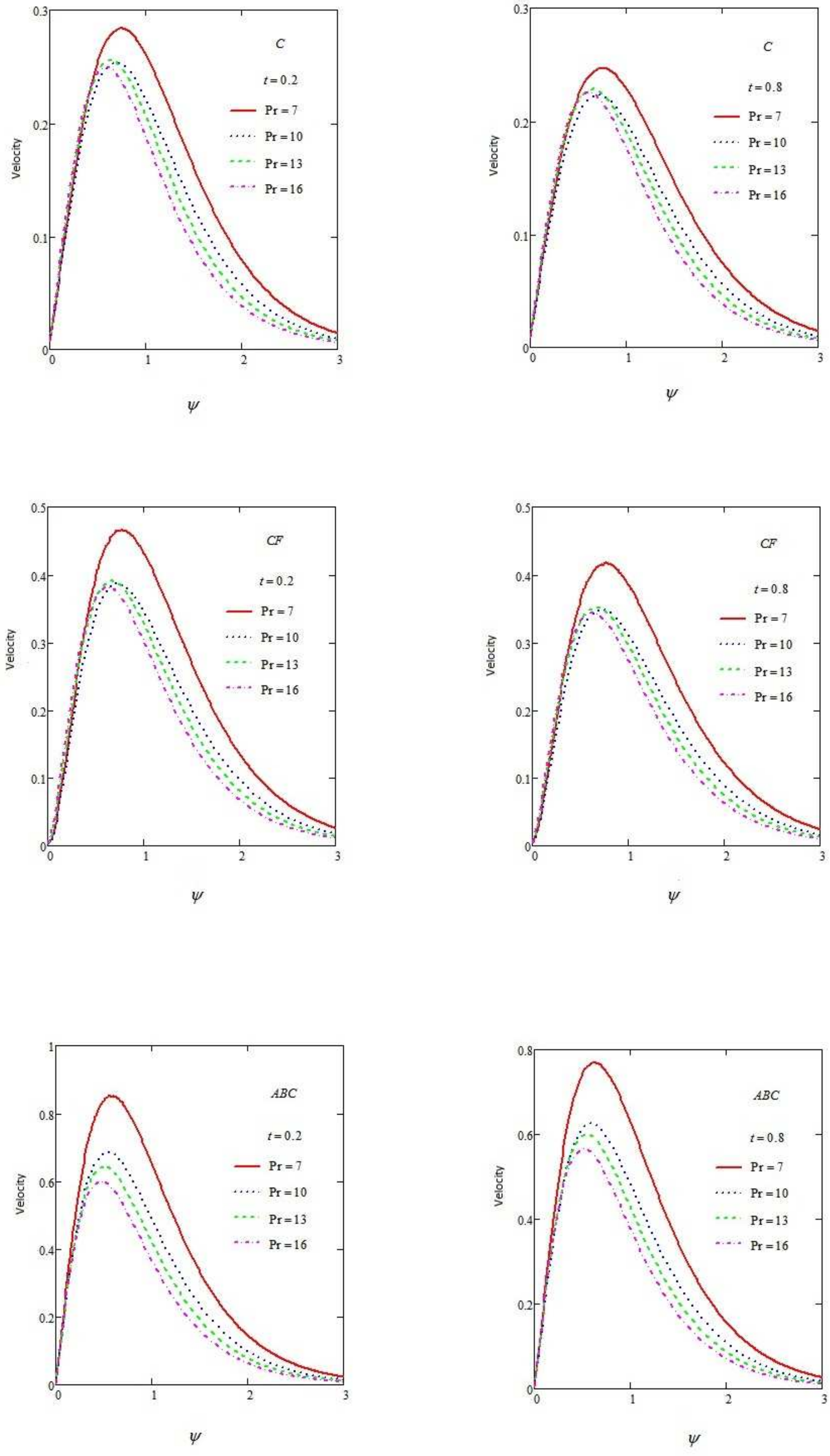

Fig. 5. **Velocity curves for C, CF and ABC with variation in** Pr **where**

$$G_r = 1, M = 1, G_c = 1, Sc = 6, K_p = 0.5, K_c = 3, \alpha = 0.01, R = 3, S = 0.5, a = 0.01, \theta = \frac{\pi}{3}, \phi = \frac{\pi}{4}$$

7.2 Velocity profile for M

The impact of M can be observed through Figure (3). Velocity declined with the increase in M. Physically, the fluid flow reduces due frictional force which is directly proportional to M and hence velocity decreases. The behavior of non-integer order models in velocity for Hartmann number is the same at different times.

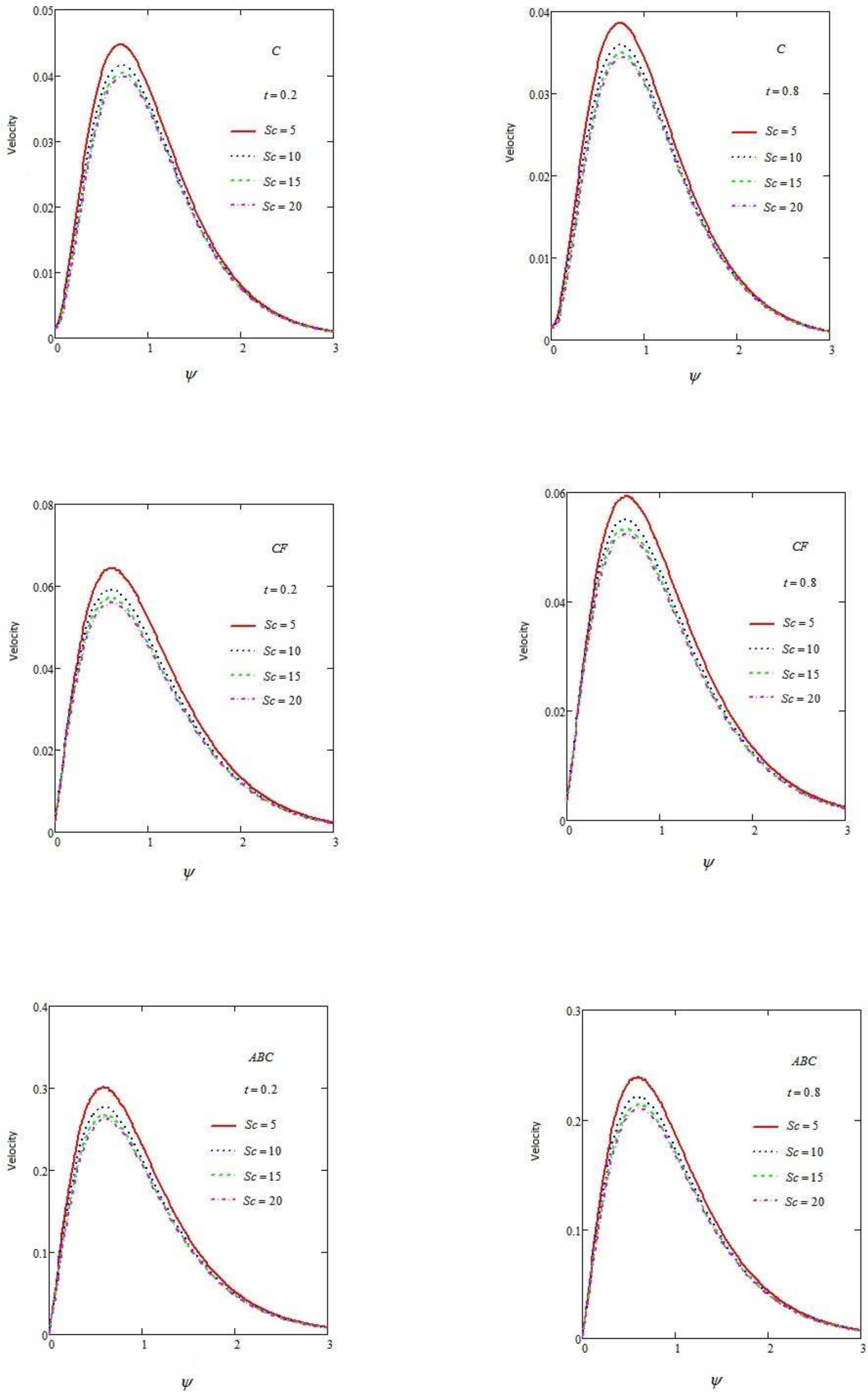

Fig. 6. Velocity curves for C, CF and ABC with variation in Sc where

$$G_r = 1, \Pr = 8, G_c = 1, M = 1, K_p = 0.5, K_c = 3, \alpha = 0.01, R = 3, S = 0.5, a = 0.01, \theta = \frac{\pi}{3}, \phi = \frac{\pi}{4}$$

7.3 Velocity profile for G_r

Figure (4) presents that with the increase in G_r, raises velocity. Physically, rise in temperature accelerates buoyancy forces, as a result velocity increases. Clearly, velocity is highest for the ABC model.

7.4 Velocity profile for Pr

Figure (5) focuses the significance of Pr in variation of fluid velocity. Fluid flow decays for when Pr accelerates. Physically, thermal conductivity associated with Pr which leads to decline due to which the viscosity enhance and resultantly, velocity decays.

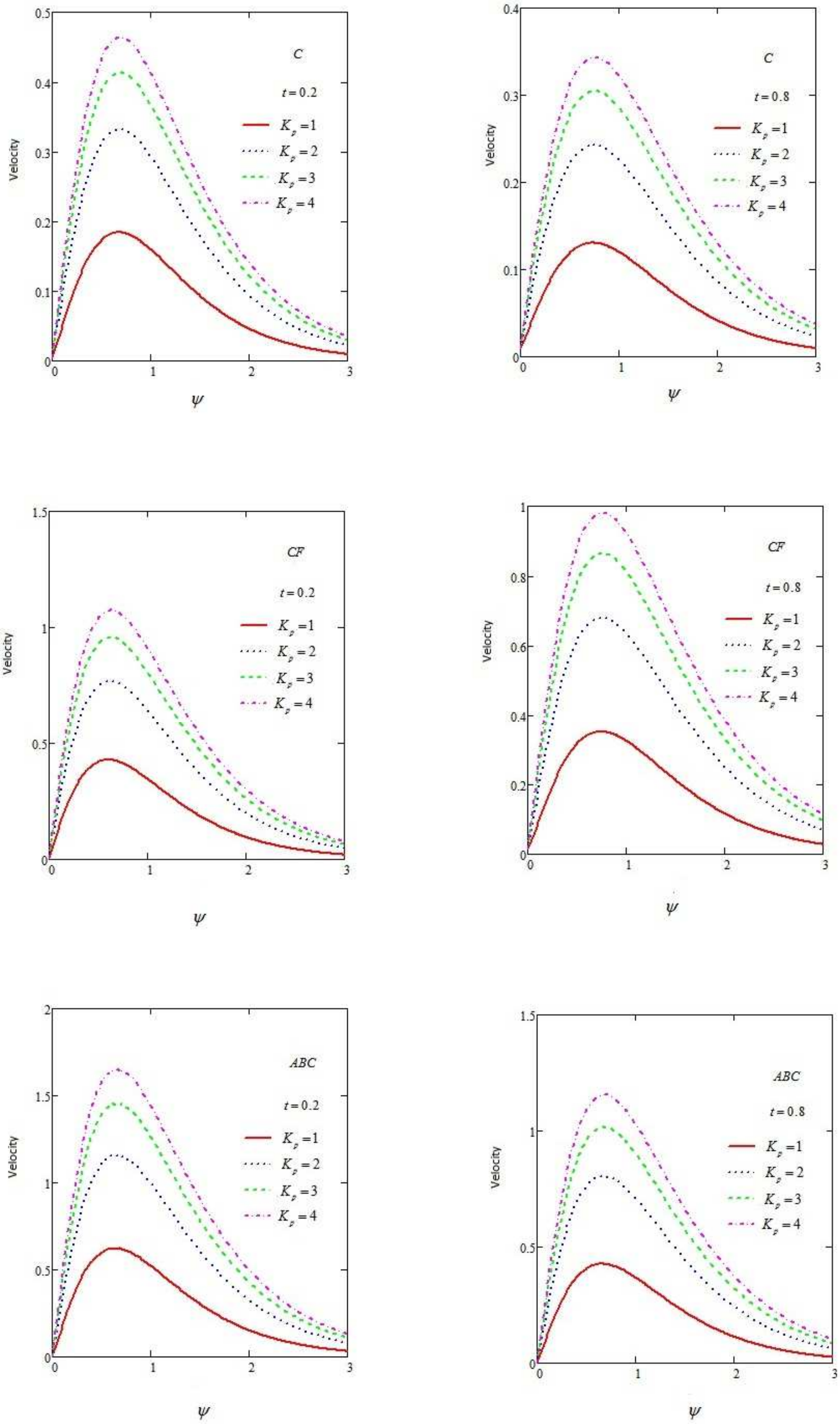

Fig. 7. Velocity curves for C, CF and ABC with variation in K_p where

$$G_r = 1, \mathrm{Pr} = 8, G_c = 1, \mathrm{Sc} = 6, M = 1, K_c = 3, \alpha = 0.01, R = 3, S = 0.5, a = 0.01, \theta = \frac{\pi}{3}, \phi = \frac{\pi}{4}$$

7.5 Velocity profile for Sc

The consequence of Sc variation on velocity profile is featured in Figure (6). It is espied that enlargement in values of Sc results in deceleration of velocity field. The physical logic of decline in velocity is the reduction molecular diffusivity due to enlargement in Sc.

7.6 Velocity profile for K_p

Figure (7) analyzes the impact of the porosity K_p on velocity. Velocity profiles increase when we raise porosity. As we compare C, CF and ABC curves we can see that velocity is maximum for ABC.

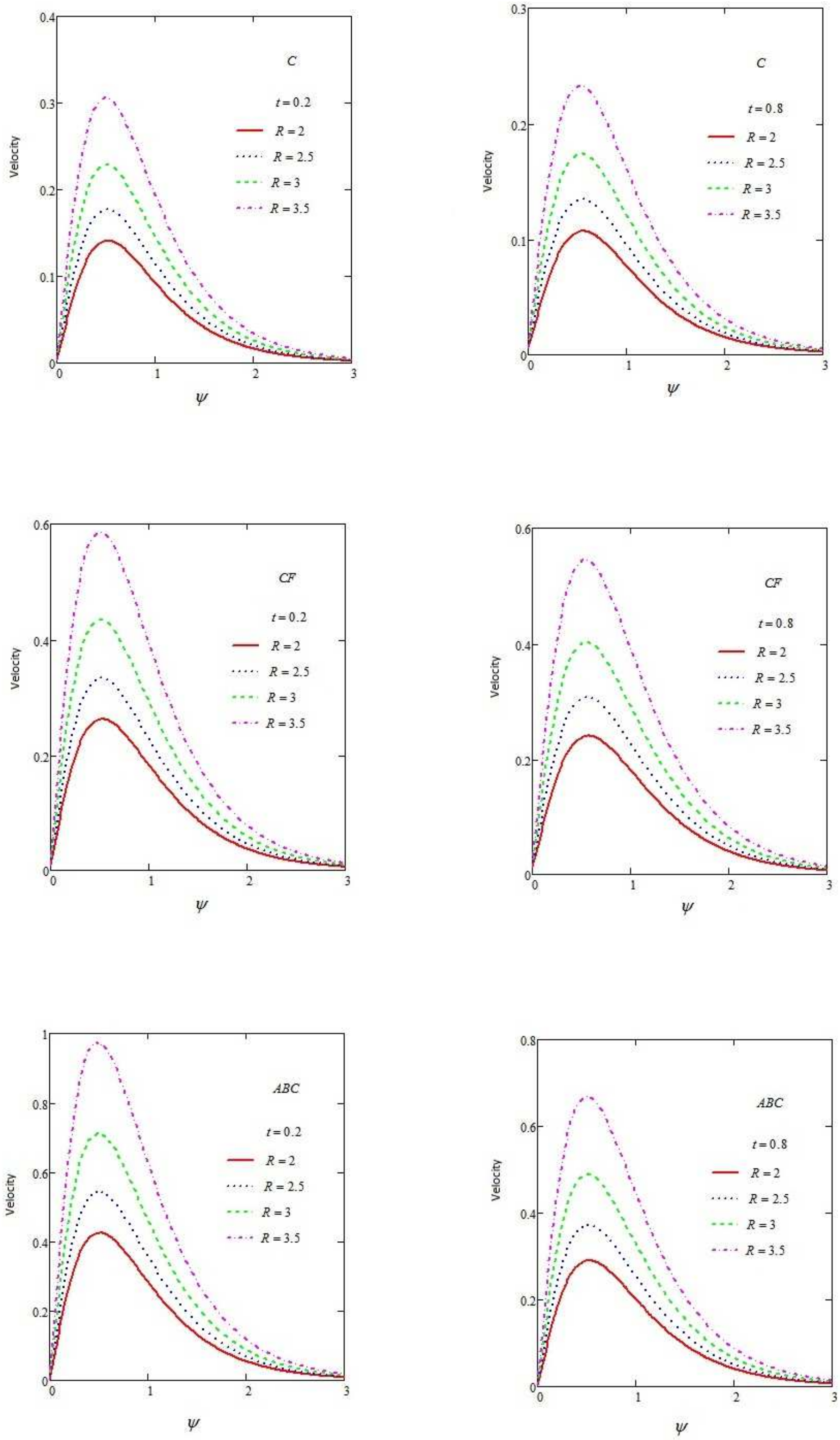

Fig. 8. Velocity curves for C, CF and ABC with variation in R where

$$G_r = 1, \Pr = 8, G_c = 1, Sc = 6, K_p = 0.5, K_c = 3, \alpha = 0.01, M = 1, S = 0.5, a = 0.01, \theta = \frac{\pi}{3}, \phi = \frac{\pi}{4}$$

7.7 Velocity profile for R

Figure (8) illustrates impact of radiation parameter on velocity profile. Radiation parameter increases the fluid velocity. Physically, thermal buoyancy force reduces by increasing radiation due to which thermal boundary layer become thin and hence velocity becomes high. While comparing the effect of R on velocity for fractional time derivatives, clearly in case of C velocity is less as compared to CF and ABC.

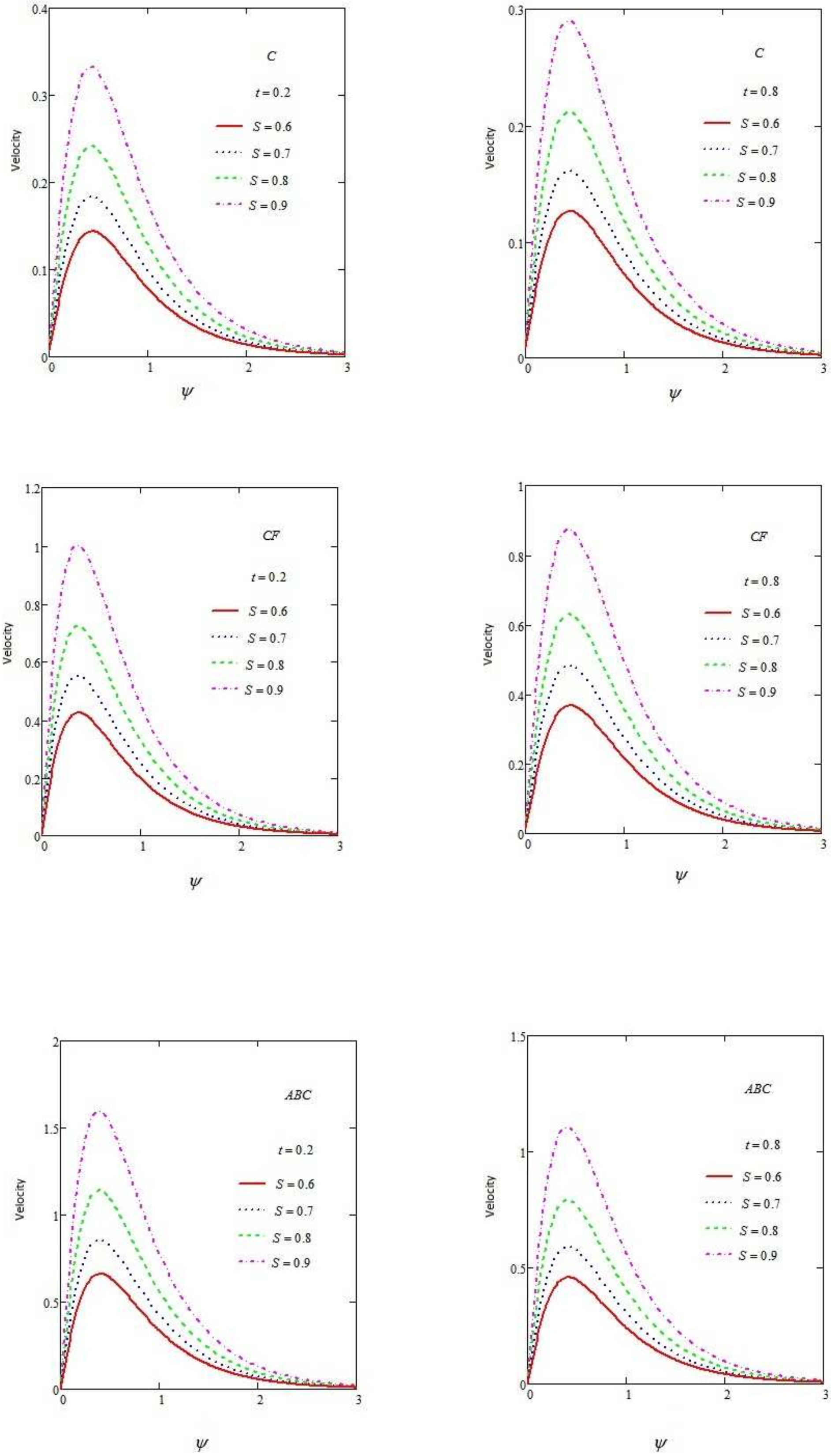

Fig. 9. Velocity curves for C, CF and ABC with variation in S where

$$G_r = 1, \Pr = 8, G_c = 1, Sc = 6, K_p = 0.5, K_c = 3, \alpha = 0.01, R = 3, M = 1, a = 0.01, \theta = \frac{\pi}{3}, \phi = \frac{\pi}{4}$$

7.8 Velocity profile for S

Velocity curves for heat source parameter S can be observed through Figure (9). Physically, by increasing the heat source more heat is generated due to which temperature increases and hence velocity is enhanced. Velocity raises under the influence of S for all fractional models.

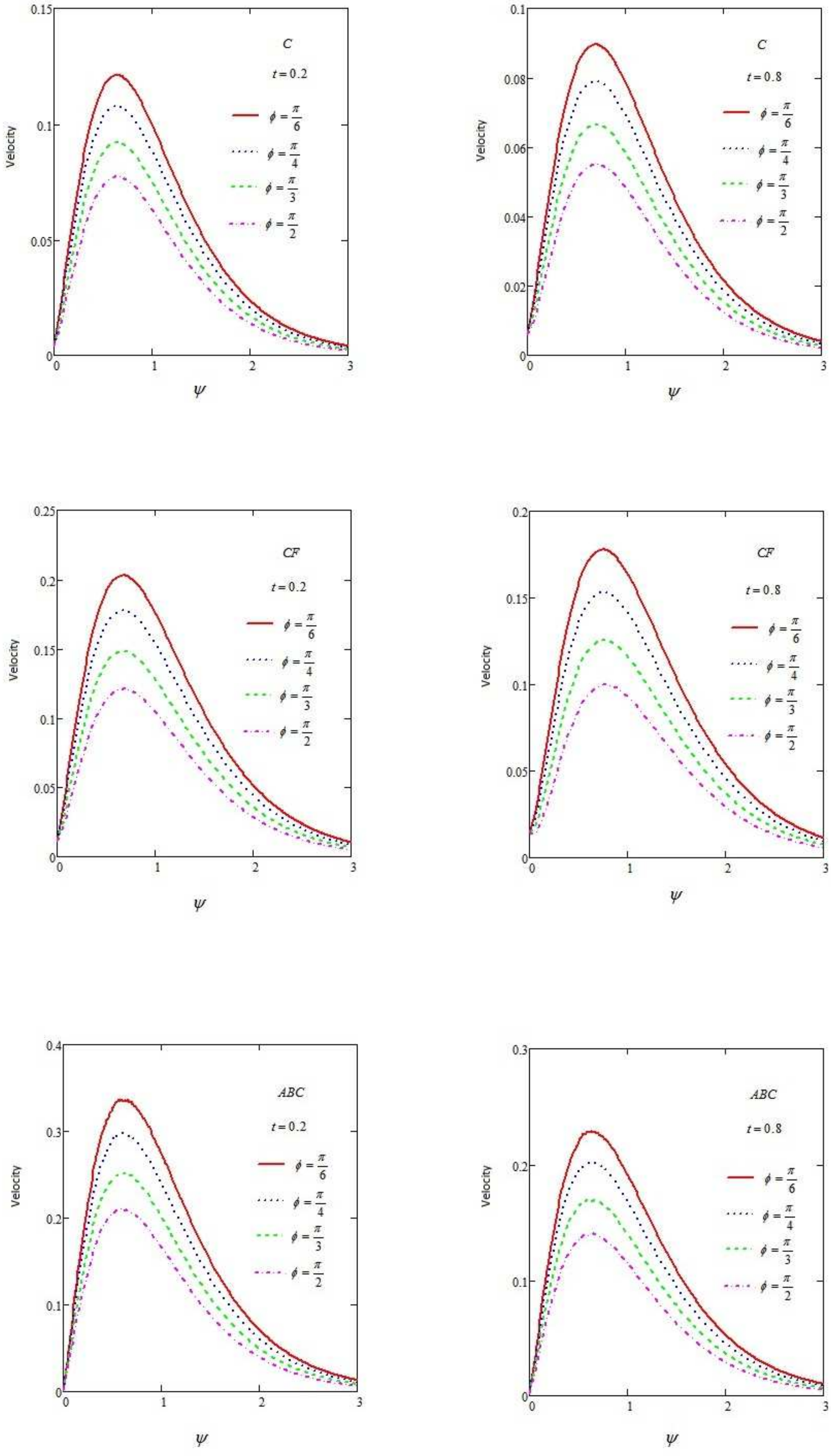

Fig. 10. Velocity curves for C, CF and ABC with variation in ϕ where

$$G_r = 1, \Pr = 8, G_c = 1, Sc = 6, K_p = 0.5, K_c = 3, \alpha = 0.01, R = 3, S = 0.5, a = 0.01, M = 1, \theta = \frac{\pi}{3}$$

7.9 Velocity profile for ϕ

Figure (10) shows that rise in angle of inclination causes reduction in velocity. Velocity reduces for ϕ for all fractional models.

7.10 Temperature profile for $\alpha, \Pr, R$

Figures (11), (12), and (13) highlights the behavior of temperature curves for fractional parameter, Prandtl number and radiation parameter. With the increase in $\alpha, \Pr, R$ temperature decreases. Temperature is least for Caputo and maximum for ABC.

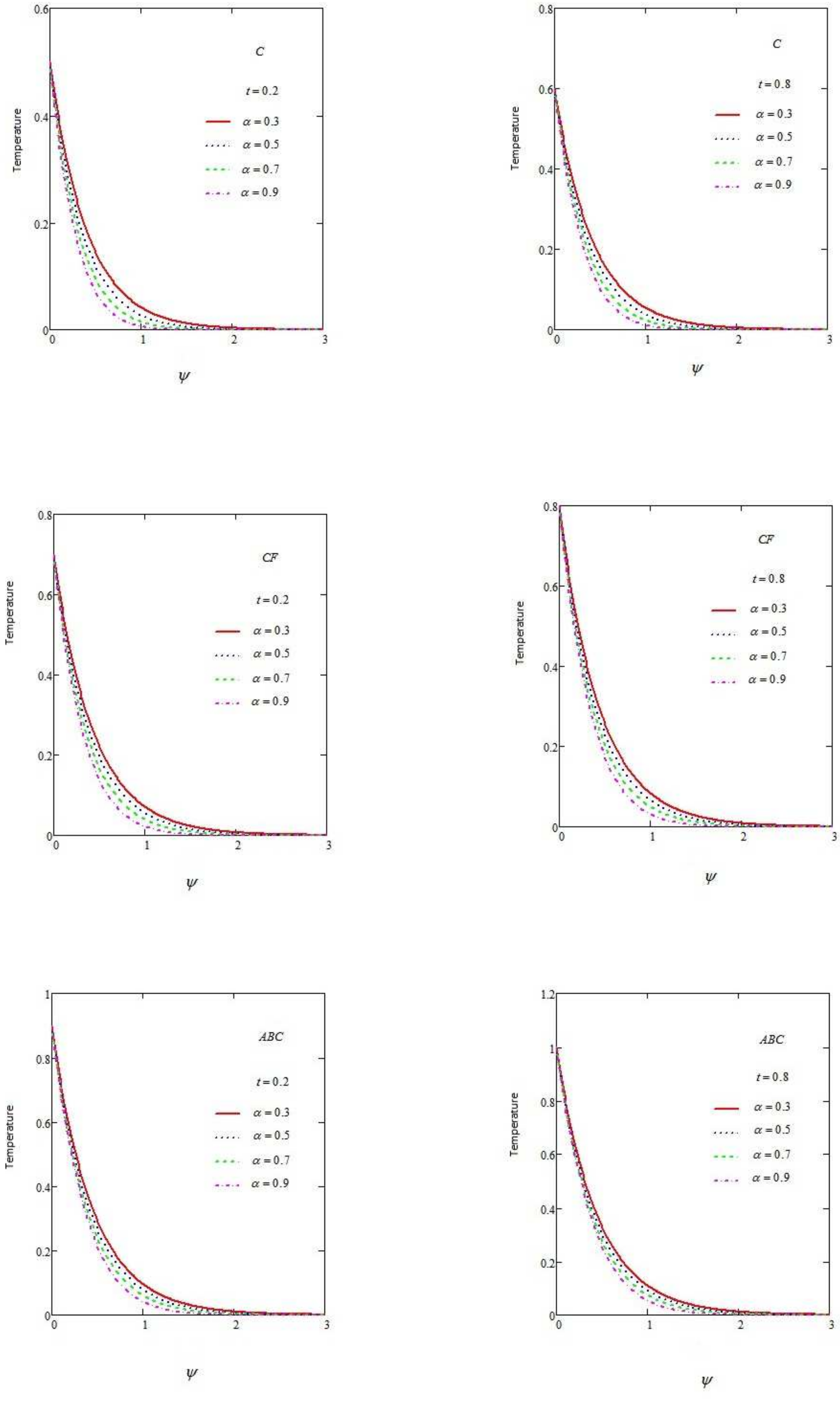

Fig. 11. Temperature curves for C, CF and ABC with variation in α where

$$G_r = 1, \Pr = 8, G_c = 1, Sc = 6, K_p = 0.5, K_c = 3, M = 1, R = 3, S = 0.5, a = 0.01, \theta = \frac{\pi}{3}, \phi = \frac{\pi}{4}$$

7.11 Concentration profile for α, Sc, K_c

Figures (14), (15) and (16) represents the impact of α, Sc, K_c on concentration field. Clearly, concentration reduces for all models. With the increment in values of Sc, molecular diffusivity becomes less so concentration decreases. Graphical behavior of concentration is prominent for ABC as in comparison with other two models.

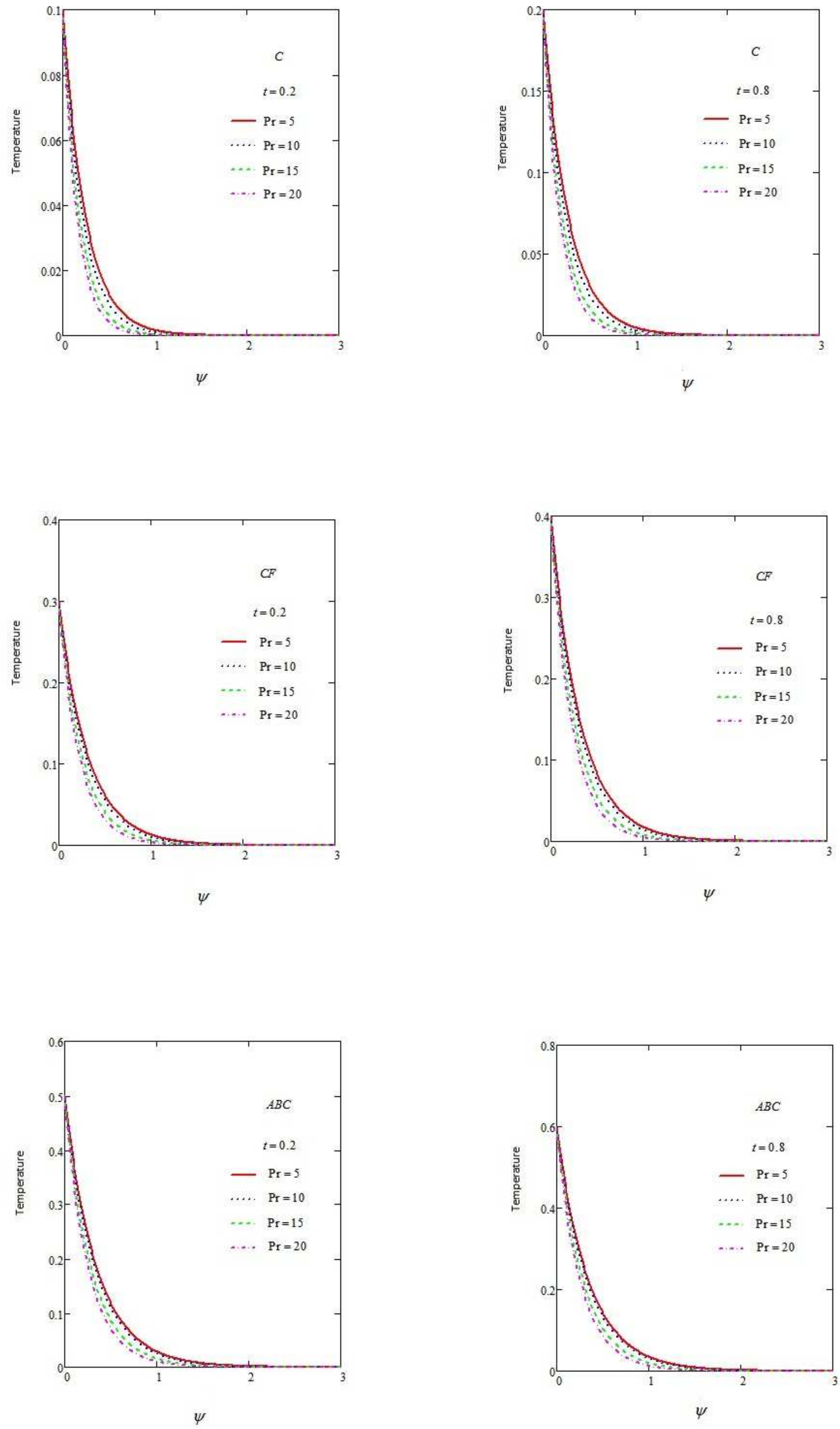

Fig. 12. Temperature curves for C, CF and ABC with variation in Pr where

$$G_r = 1, M = 1, G_c = 1, Sc = 6, K_p = 0.5, K_c = 3, \alpha = 0.01, R = 3, S = 0.5, a = 0.01, \theta = \frac{\pi}{3}, \phi = \frac{\pi}{4}$$

In Table 1, inversion algorithm is used to compute velocity for all fractional models for ϕ. Velocity showing increasing behavior for all models. Table 2, and 3 interpret numerical calculations for Nu corresponding to Pr are Sh corresponding to Sc respectively via Stehfest's and Tzou's algorithms. Heat and mass transfer rate is high for the ABC model as compared to the rest of the two models.

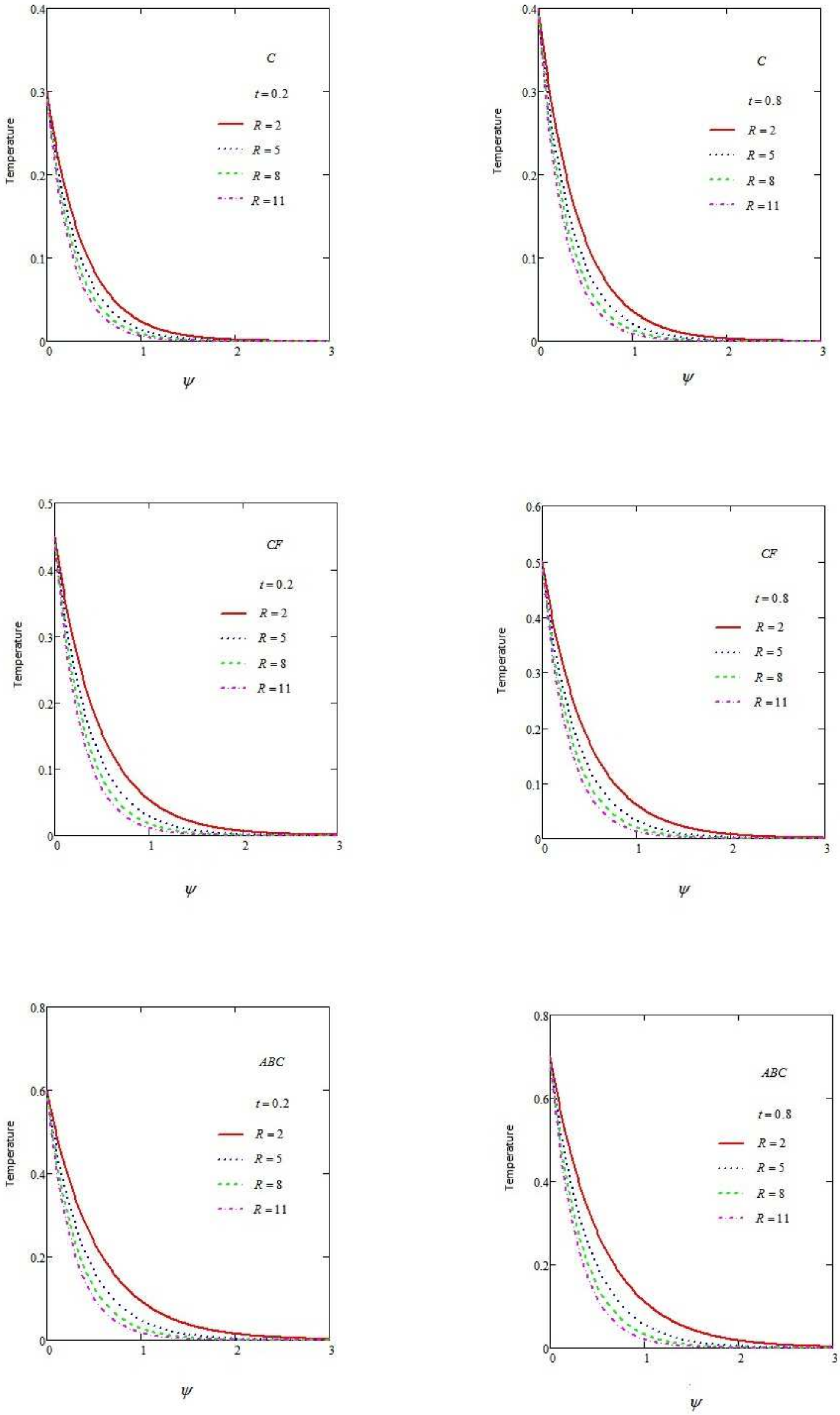

Fig. 13. Temperature curves for C, CF and ABC with variation in R where

$$G_r = 1, Pr = 8, G_c = 1, Sc = 6, K_p = 0.5, K_c = 3, \alpha = 0.01, M = 1, S = 0.5, a = 0.01, \theta = \frac{\pi}{3}, \phi = \frac{\pi}{4}$$

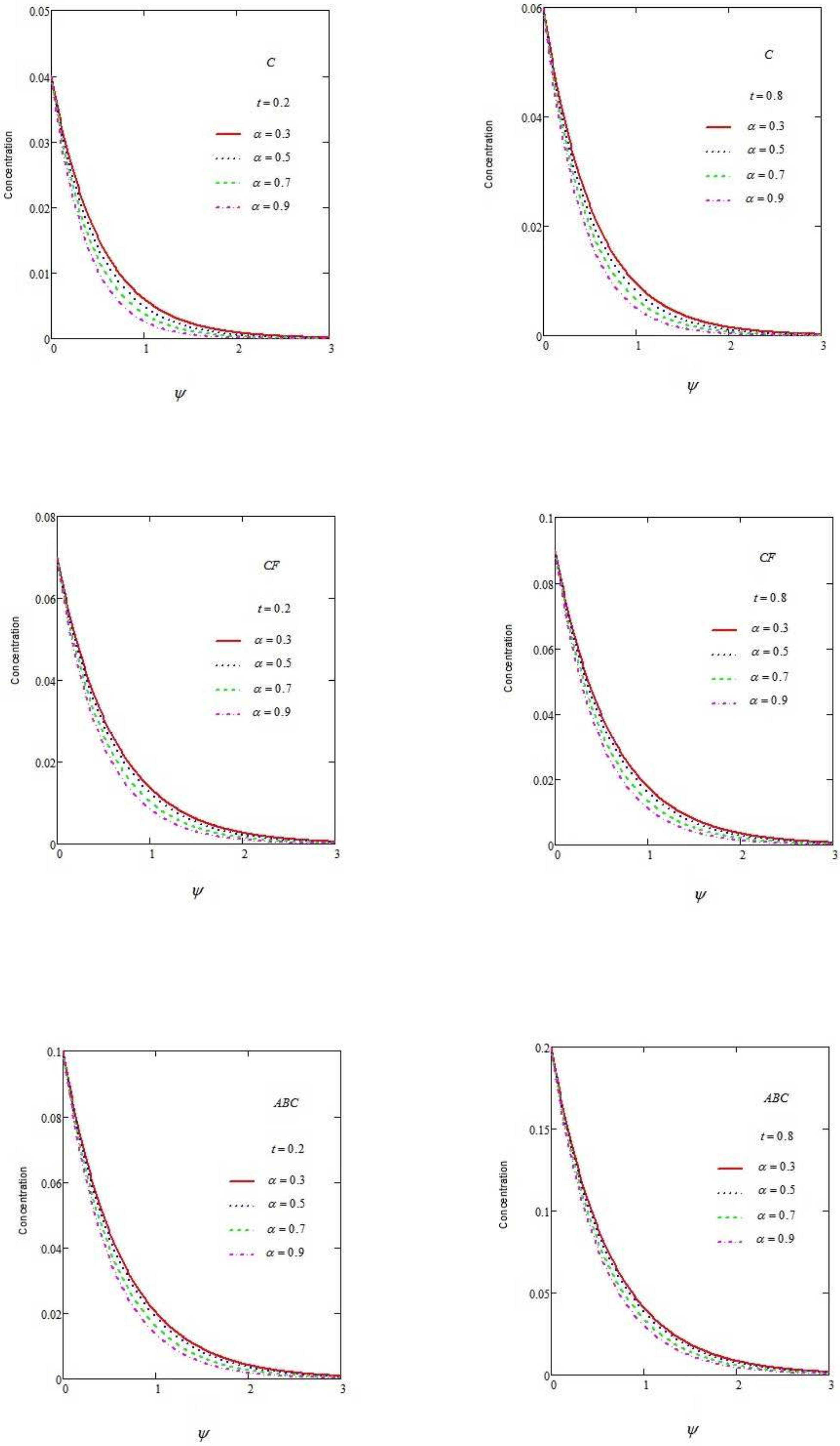

Fig. 14. Concentration curves for C, CF and ABC with variation in α where

$$G_r = 1, \Pr = 8, G_c = 1, Sc = 6, K_p = 0.5, K_c = 3, M = 1, R = 3, S = 0.5, a = 0.01, \theta = \frac{\pi}{3}, \phi = \frac{\pi}{4}$$

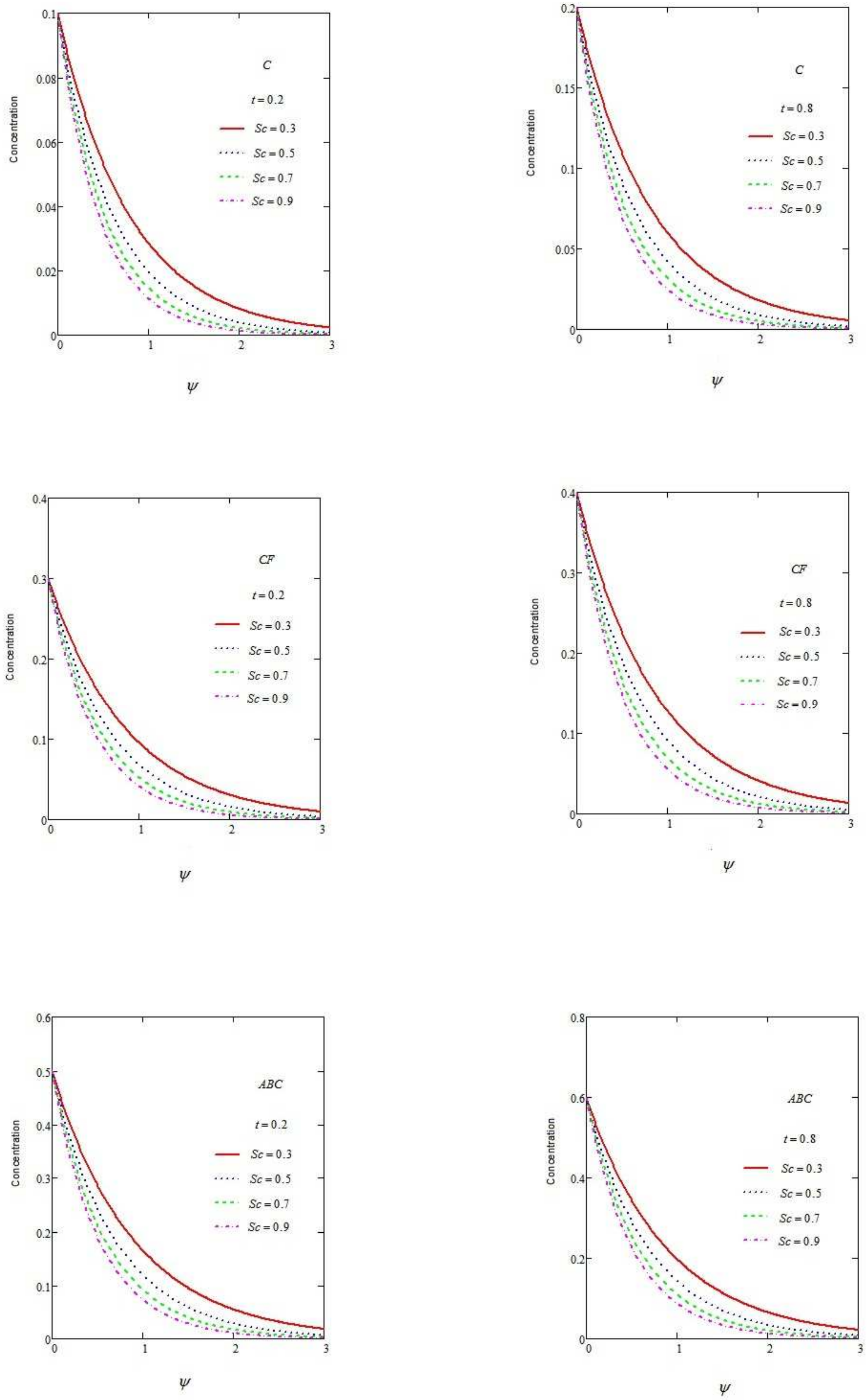

Fig. 15. Concentration curves for C, CF and ABC with variation in Sc where

$$G_r = 1, \Pr = 8, G_c = 1, M = 1, K_p = 0.5, K_c = 3, \alpha = 0.01, R = 3, S = 0.5, a = 0.01, \theta = \frac{\pi}{3}, \phi = \frac{\pi}{4}$$

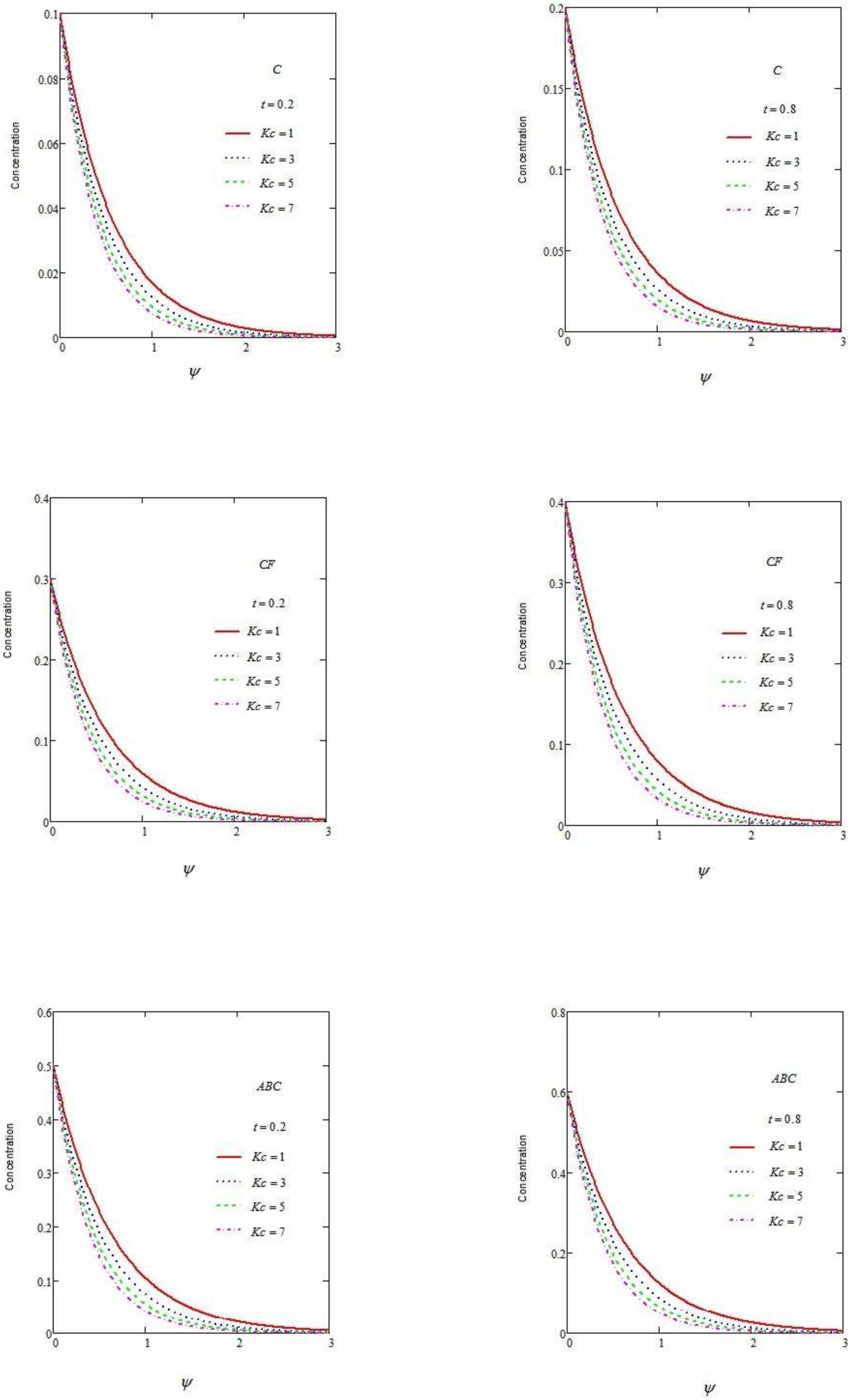

Fig. 16. Velocity curves for C, CF and ABC with variation in K_c where

$$G_r = 1, \Pr = 8, G_c = 1, Sc = 6, K_p = 0.5, M = 1, \alpha = 0.01, R = 3, S = 0.5, a = 0.01, \theta = \frac{\pi}{3}, \phi = \frac{\pi}{4}$$

Table 1. Calculations for velocity by numerical inversion Laplace transform for Stehfest's and Tzou's

ψ	Velocity C (Stehfest's)	Velocity C (Tzou's)	Velocity CF (Stehfest's)	Velocity CF (Tzou's)	Velocity ABC (Stehfest's)	Velocity ABC (Tzou's)
0.3	0.218	0.206	0.373	0.319	0.334	0.328
0.6	0.213	0.199	0.283	0.257	0.326	0.314
0.9	0.186	0.172	0.209	0.143	0.302	0.294
1.3	0.152	0.135	0.152	0.141	0.285	0.255
1.6	0.118	0.103	0.118	0.108	0.238	0.138
1.9	0.089	0.056	0.076	0.047	0.179	0.163
2.2	0.065	0.039	0.053	0.062	0.135	0.121
2.5	0.046	0.025	0.037	0.031	0.115	0.105
2.8	0.033	0.020	0.026	0.021	0.073	0.067

Table 2. Calculations for Nusselt number by numerical inversion Laplace transform for Stehfest's and Tzou's

Pr	*Nu* C (Stehfest's)	*Nu* C (Tzou's)	*Nu* CF (Stehfest's)	*Nu* CF (Tzou's)	*Nu* ABC (Stehfest's)	*Nu* ABC (Tzou's)
1	0.214	0.210	0.234	0.206	0.282	0.265
2	0.284	0.243	0.308	0.301	0.385	0.351
3	0.344	0.363	0.371	0.353	0.466	0.401
4	0.387	0.371	0.422	0.414	0.535	0.519
5	0.433	0.442	0.469	0.436	0.596	0.552
6	0.468	0.451	0.512	0.503	0.651	0.632
7	0.504	0.516	0.551	0.547	0.732	0.709
9	0.537	0.520	0.588	0.564	0.749	0.721
9	0.569	0.542	0.622	0.619	0.794	0.741
10	0.576	0.589	0.655	0.649	0.836	0.812

Table 3. Calculations for Sherwood number by numerical inversion Laplace transform for Stehfest's and Tzou's

Sc	*Sh* C (Stehfest's)	*Sh* C (Tzou's)	*Sh* CF (Stehfest's)	*Sh* CF (Tzou's)	*Sh* ABC (Stehfest's)	*Sh* ABC (Tzou's)
0.3	0.117	0.113	0.123	0.120	0.128	0.122
0.6	0.166	0.144	0.171	0.167	0.181	0.154
0.9	0.213	0.179	0.203	0.185	0.222	0.206
1.3	0.234	0.215	0.242	0.218	0.256	0.232
1.6	0.262	0.244	0.271	0.239	0.286	0.258
1.9	0.287	0.258	0.296	0.268	0.314	0.289
2.2	0.311	0.279	0.322	0.288	0.339	0.319
2.5	0.332	0.301	0.342	0.307	0.362	0.325
2.8	0.352	0.319	0.363	0.325	0.374	0.385

8. Conclusion

The study of natural convective flow with chemical reaction and thermal radiation past a moving slanted infinite plate and slanted magnetic field has been discussed via integer and non-integer models. The solutions of model equations are developedthrough Laplace transform and inversion algoritnm. The main focus is the comparison for different fractional models. From our general results, some results can be deduced from literature. Velocity curves are showing increasing behavior for fractional parameter α whereas temperature and concentration curves are showing decreasing behavior for α. There is decline in velocity as M, Sc and φ increase for integer order models. Velocity enhances for K_p, G_r and S for all fractional models. Temperature and velocity have the same behavior for Pr while both have opposite behavior for R in all cases. Concentration declines while we raise the value of Sc and K_c. Nusselt number for Pr and Sherwood number for Sc increase for all non-integer order models.

Author Contributions

N. Iftikhar solved the proposed mathematical model and verify the required results; D. Baleanu ploted the graphs using software and verify the results present in literature; M.B. Riaz proposed the problem, initiated the conceptualization, developed the mathematical modeling and examined the theory valiadation; S.M. Husnine edit the paper. Final version of the article is approved by all authors.

Acknowledgments

Authors are appreciated and thankful for support of this research article.

Conflict of Interest

The authors declared no potential conflicts of interest with respect to the research, authorship, and publication of this article.

Funding

There is no funding received by authors for this article.

Nomenclature

υ	Kinematic viscosity	α	Fractional parameter
g	Acceleration due to gravity	t	Time
ρ	Fluid denisty	Pr	Prandtl number
C_p	Specific heat	Sc	Schmidt number
β_C	Volumetric coefficient of expansion for mass transfer	λ	Relaxation time
β_T	Volumetric coefficient of thermal expansion	σ	Electrical conductivity of the fluid
μ	Dynamic viscosity	B_0	Magnetic field
a^*	Absorption constant	M	Hartmann number
a	Dimensionless acceleration parameter	D	Molecular diffusivity of chemical
G_r	Thermal Grashof number	K	Thermal conductivity
G_c	Mass Grashof number	q_r	Relative heat flux
R	Radiation parameter	K_p	Porosity parameter
W	Velocity of the fluid	K_c	Chemical reaction parameter
T	Fluid temperature	S	Heat source parameter
C	Fluid concentration	C_w	Concentration on the plate
m	Laplace transforms parameter	C_∞	Concentration of the fluid far away from the plate
T_w	Temperature of the plate	θ	Angle of inclination of the plate
T_∞	Temperature of fluid far away from the plate	ϕ	Angle of inclination of applied magnetic field

References

[1] Jha, B.K., MHD free-convection and mass-transform flow through a porous medium. *Astrophysics and Space science,* 2, 1991, 283 – 289.
[2] Kamel, M.H., Unsteady MHD convection through porous medium with combined heat and mass transfer with heat source/sink. *Energy Conversion and Management,* 4, 2001, 393 – 405.
[3] Ibrahim, F.S., Hassanien, I.A., Bakr, A.A., Unsteady magnetohydrodynamic micropolar fluid flow and heat transfer over a vertical porous plate through a porous medium in the presence of thermal and mass diffusion with a constant heat source. *Canadian Journal of Physics,* 10, 2004, 775 – 790.
[4] Eldabe, N.T.M., Elbashbeshy, E.M.A., Hasanin, W.S.A., Elsaid, E.M., Unsteady motion of MHD viscous incompressible fluid with heat and mass transfer through porous medium near a moving vertical plate. *International Journal of Energy and Technology*, 3, 2011, 1 – 11.
[5] Doungmo Goufo, E. F., Mathematical analysis of peculiar behavior by chaotic, fractional and strange multiwing attractors. *International Journal of Bifurcation and Chaos,* 28, 2018, 1850125.
[6] Goufo E. F., Application of the Caputo-Fabrizio Fractional Derivative without Singular Kernel to Korteweg-de Vries-Burgers Equation. *Mathematical Modelling and Analysis,* 21, 2016, 188 – 198.
[7] Goufo, E.F., On chaotic models with hidden attractors in fractional calculus above power law. *Chaos, Solitons and Fractals*, 127, 2019, 24 – 30.
[8] Owusu, K.F. Goufo, E. F, Mugisha, S., Modelling intracellular delay and therapy interruptions within Ghanaian HIV population. *Advances in Difference Equations,* 1, 2020, 1 – 9.
[9] Khan, I., Saeed, S.T., Riaz, M.B., Abro, K.A., Husnine, S.M., Nissar, K.S., Influence in a Darcy's Medium with Heat Production and Radiation on MHD Convection Flow via Modern Fractional Approach. *Journal of Materials Research and Technology,* 5, 9, 2020, 10016 – 10030.
[10] Riaz, M.B., Saeed, S.T., Baleanu, D., Ghalib, M., Computational results with non-singular & non-local kernel flow of viscous fluid in vertical permeable medium with variant temperature. *Frontier in Physics,* 8, 2020, 275.
[11] Riaz, M.B., Saeed, S.T., Baleanu, D., Role of Magnetic field on the Dynamical Analysis of Second Grade Fluid: An Optimal Solution subject to Non-integer Differentiable Operators. *Journal of Applied and Computational Mechanics,* 6(SI), 2020, 1475 – 1489.
[12] Song, D.Y., Jiang, T.Q., Study on the constitutive equation with fractional derivative for the viscoelastic fluids modified Jeffreys model and its application. *Rheologica Acta,* 5, 37, 1998, 512 – 517.
[13] Riaz, M.B., Siddiqui, M., Saeed, S.T.,Atangana, A., MHD Oldroyd-B Fluid with Slip Condition in view of Local and Nonlocal Kernels, *Journal of Applied and Computational Mechanics,* 6(SI), 2020, 1540 – 1551.
[14] Podlubny, I., Fractional differential equations: an introduction to fractional derivatives, fractional differential equations, to methods of their solution and some of their applications. *Elsevier,* 1998.
[15] Wenchang, T., Wenxiao, P., Mingyu, X., A note on unsteady flows of a viscoelastic fluid with the fractional Maxwell model between two parallel plates. *International Journal of Non-Linear Mechanics,* 5, 38, 2003, 645 – 650.
[16] Riaz, M.B., Iftikhar, N., A comparative study of heat transfer analysis of MHD Maxwell fluid in view of local and nonlocal differential operators. *Chaos, Solitons and Fractals*, 132, 2020, 109556.
[17] Riaz, M.B., Saeed, S.T., Comprehensive analysis of integer order, Caputo-fabrizio and Atangana-Baleanu fractional time derivative for MHD Oldroyd-B fluid with slip effect and time dependent boundary condition. *Discrete and Continuous Dynamical Systems,* 2020, Accepted.
[18] Saeed, S.T., Riaz, M.B., Baleanu, D., Abro, K.A., A Mathematical Study of Natural Convection Flow Through a Channel with non-singular Kernels: An Application to Transport Phenomena. *Alexandria Engineering Journal, 59,* 2020, 2269 – 2281.
[19] Riaz, M.B., Atanganaa, A., Saeed, S.T., *MHD free convection flow over a vertical plate with ramped wall temperature and chemical reaction in view of non-singular kernel*. Wiley, 2020, 253 – 279.
[20] Qi, H., Xu, M., Unsteady flow of viscoelastic fluid with fractional Maxwell model in a channel. *Mechanics Research Communications,* 2, 34, 2007, 210 – 212.
[21] Riaz, M.B., Atangana, A., Abdeljawad, T., Local and non-local differential operators: A comparative study of heat and mass transfer in MHD Oldroyd-B fluid with ramped wall temperature. *Fractal*, 2020, https://doi.org/10.1142/S0218348X20400332.
[22] Riaz, M.B., Atangana, A., Iftikhar, N., Heat and mass transfer in Maxwell fluid in view of local and non-local differential operators. *Journal of Thermal Analysis and Calorimetry,* 2020.
[23] Zafar, A.A., Riaz, M.B., Shah, N.A., Imran, M.A., Influence of non-integer derivatives on unsteady unidirectional motions of an Oldroyd-B fluid with generalized boundary condition. *The European Physical Journal Plus,* 3, 133, 2018, 1 – 13.
[24] Abro, K.A., Khan, I., Gomez-Aguilar, J.F., A mathematical analysis of a circular pipe in rate type fluid via Hankel transform. *The European Physical Journal Plus,* 10, 133, 2018, 397.
[25] Umemura, A., Law, C.K., Natural-convection boundary-layer flow over a heated plate with arbitrary inclination. *Journal of Fluid Mechanics*, 219, 1990, 571 – 584.
[26] Pattnaik, J.R., Dash, G.C., Singh, S., Radiation and mass transfer effects on MHD flow through porous medium past an exponentially accelerated inclined plate with variable temperature. *Ain Shams Engineering Journal,* 1, 8, 2017, 67 – 75.
[27] Nandkeolyar, R., Das, M., MHD free convective radiative flow past a flat plate with ramped temperature in the presence of an inclined magnetic field. *Computational and Applied Mathematics,* 34, 1, 2015, 109 – 123.
[28] Endalew, M.F., Nayak, A., Thermal radiation and inclined magnetic field effects on MHD flow past a linearly accelerated inclined plate in a porous medium with variable temperature. *Heat Transfer Asian Research,* 1, 48, 2019, 42 – 61.

[29] Uddin, Z., Kumar, M., Unsteady free convection in a fluid past an inclined plate immersed in a porous medium. *Computer Modelling and New Technologies,* 3, 14, 2010, 41 – 47.
[30] Ali, F., Khan, I., Shafie, S., Conjugate effects of heat and mass transfer on MHD free convection flow over an inclined plate embedded in a porous medium. *PLoS One,* 6, 8, 2013, 65223.
[31] Makinde, O.D., Heat and mass transfer by MHD mixed convection stagnation point flow toward a vertical plate embedded in a highly porous medium with radiation and internal heat generation. *Meccanica,* 5, 47, 2012, 1173 – 1184.
[32] Khalid, A., Khan, I., Khan, A., Shafie, S., Unsteady MHD free convection flow of Casson fluid past over an oscillating vertical plate embedded in a porous medium. *Engineering Science and Technology, an International Journal,* 3, 18, 2015, 309 – 317.
[33] Iftikhar, N., Husnine, S.M., Riaz, M.B., Heat and mass transfer in MHD Maxwell fluid over an infinite vertical plate. *Journal of Prime Research in Mathematics*, 15, 2019, 63 – 80.
[34] Riaz, M.B., Imran, M.A., Shabbir, K., Analytic solutions of Oldroyd-B fluids with fractional derivatives in a circular duct that applies a constant couple. *Alexendria Engineering Journal*, 4, 55, 2016, 3267 – 3275.
[35] Abro, K.A., A Fractional and Analytic Investigation of Thermo-Diffusion Process on Free Convection Flow: An Application to Surface Modification Technology. *The European Physical Journal Plus,* 1, 31, 2020, 135.
[36] Abro, K.A., Atangana, A., A comparative study of convective fluid motion in rotating cavity via Atangana–Baleanu and Caputo–Fabrizio fractal–fractional differentiation. *The European Physical Journal Plus,* 2, 135, 2020, 226
[37] Shah, N.A., Elnaqeeb, T., Wang, S., Effects of Dufour and fractional derivative on unsteady natural convection flow over an infinite vertical plate with constant heat and mass fluxes. *Computational and Applied Mathematics,* 4, 37, 2018, 4931-4943.
[38] Khan, A., Abro, K. A., Tassaddiq, A., Khan, I., Atangana Baleanu and Caputo Fabrizio analysis of fractional derivatives for heat and mass transfer of second grade fluids over a vertical plate: a comparative study. *Entropy,* 8, 19, 2017, 279.
[39] Tassaddiq, A., MHD flow of a fractional second grade fluid over an inclined heated plate. *Chaos Solitons & Fractals,* 1, 123, 2019, 341 – 346.
[40] Shah, N. A., Ahmed, N., Elnaqeeb, T., Rashidi, M. M., Magnetohydrodynamic free convection flows with thermal memory over a moving vertical plate in porous medium. *Journal of Applied and Computational Mechanics,* 1, 5, 2019, 150-161.
[41] Sheikh, N.A., Ali, F., Khan, I., Saqib, M., A modern approach of Caputo Fabrizi time-fractional derivative to MHD free convection flow of generalized second grade fluid in a porous medium. *Neural Computing and Applications,* 6, 2018, 1865 – 1875.
[42] Imran, M.A., Aleem, M., Riaz, M.B., Ali, R., Khan, I., A comprehensive report on convective flow of fractional (ABC) and (CF) MHD viscous fluid subject to generalized boundary conditions. *Chaos, Solitons & Fractals,* 118, 2018, 274 – 289.
[43] Ahmad, M., Imran, M.A., Aleem, M., Khan, I., A comparative study and analysis of natural convection flow of MHD non-Newtonian fluid in the presence of heat source and first-order chemical reaction. *Journal of Thermal Analysis and Calorimetry,* 5, 137, 2019 , 1783 – 1796.
[44] Caputo, M., Fabrizio, M., A New Definition of Fractional Derivative Without Singular Kernel, *Progress in Fractional Differentiation and Applications*, 2, 1, 2015, 1 – 11.
[45] Atangana, A., On the new fractional derivative and application to nonlinear Fisher's reaction–diffusion equation. *Applied Mathematics and Computation*, 273, 2016, 948 – 956.
[46] Atangana, A., Koca, I., New direction in fractional differentiation. *Mathematics in Natural Science*, 1, 2017, 18–25.
[47] Fatecau, C., Zafar, A.A., Vieru, D., Awrejcewicz, J., Hydromagnetic flow over a moving plate of second grade fluids with time fractional derivatives having non-singular kernel. *Chaos Solitons & Fractals,* 130, 2020, 109454.
[48] Akgül, A., A novel method for a fractional derivative with non-local and non-singular kernel. *Chaos Solitons & Fractals,* 114, 2018, 478 – 482.
[49] Stehfest, H. A., Numerical inversion of Laplace transforms. *Communications of the ACM,* 1, 13, 1970, 47-49.
[50] Tzou, D. Y., *Macro to Microscale Heat Transfer: The Lagging Behaviour*, Washington: Taylor and Francis, 1970.

ORCID iD

Nazish Iftikhar https://orcid.org/0000-0003-1840-2262
Dumitru Baleanu https://orcid.org/0000-0002-0286-7244
Muhammad Bilal Riaz https://orcid.org/0000-0001-5153-297x
Syed Muhammad Husnine https://orcid.org/0000-0002-3237-6681

How to cite this article: Iftikhar N., Baleanu D., Riaz M.B., Husnine S.M. Heat and Mass Transfer of Natural Convective Flow with Slanted Magnetic Field via Fractional Operators, *J. Appl. Comput. Mech.*, 7(1), 2021, 189-212.
https://doi.org/10.22055/JACM.2020.34930.2514